


Process Monitoring Using Truncated Gamma Distribution

Sajid Ali ^{1,†} , Shayaan Rajput ^{1,†}, Ismail Shah ^{1,2,*,†}  and Hassan Houmani ^{3,*,†} 

- ¹ Department of Statistics, Quaid-i-Azam University, Islamabad 45320, Pakistan; sajidali@qau.edu.pk (S.A.); shayaanrajput11@gmail.com (S.R.)
- ² Department of Statistical Sciences, University of Padua, 35121 Padua, Italy
- ³ Department of Economics, School of Business, Lebanese International University-LIU, Beirut 146404, Lebanon
- * Correspondence: shah@stat.unipd.it or ishah@qau.edu.pk (I.S.); hassan.houmani@liu.edu.lb (H.H.)
- † These authors contributed equally to this work.

Abstract: The time-between-events idea is commonly used for monitoring high-quality processes. This study aims to monitor the increase and/or decrease in the process mean rapidly using a one-sided exponentially weighted moving average (EWMA) chart for the detection of upward or downward mean shifts using a truncated gamma distribution. The use of the truncation method helps to enhance and improve the sensitivity of the proposed chart. The performance of the proposed chart with known and estimated parameters is analyzed by using the run length properties, including the average run length (ARL) and standard deviation run length (SDRL), through extensive Monte Carlo simulation. The numerical results show that the proposed scheme is more sensitive than the existing ones. Finally, the chart is implemented in real-world situations to highlight the significance of the proposed chart.

Keywords: average run length; exponentially weighted moving average; standard deviation of run length; time-between-events; truncated gamma distribution

MSC: 62P30



Citation: Ali, S.; Rajput, S.; Shah, I.; Houmani, H. Process Monitoring Using Truncated Gamma Distribution. *Stats* **2023**, *6*, 1298–1322. <https://doi.org/10.3390/stats6040080>

Academic Editor: Hari Mohan Srivastava

Received: 21 September 2023
Revised: 25 November 2023
Accepted: 27 November 2023
Published: 1 December 2023



Copyright: © 2023 by the authors. Licensee MDPI, Basel, Switzerland. This article is an open access article distributed under the terms and conditions of the Creative Commons Attribution (CC BY) license (<https://creativecommons.org/licenses/by/4.0/>).

1. Introduction

The quality of a process is the ability of a product or service to meet the required criteria. Statistical process control (SPC) is a powerful approach that ensures that the process works properly and maintains its stability. The SPC identifies the assignable causes that are responsible for the variability of a process. In general, a process changes with time, no matter how much you try to control it. These changes are made either by common/natural/chance variations or by assignable causes. The variations due to natural causes are generally ignored, while assignable variations need special attention. If a process is working in the presence of a common cause, it is said to be in-control (IC); otherwise, it is said to be out-of-control (OOC). A control chart is a special tool of SPC and is used to monitor the process.

Shewhart states that the “control chart is extensively used and extremely effective for detecting substantial changes using current information in process parameters. Contrary to this approach, an exponentially weighted moving average (EWMA) chart is used to detect small changes in a process”. On the other hand, to access and analyze the performance of the control chart, one of the most effective and extensive metrics is the average run length (ARL) along with the standard deviation of the run length. The point where an OOC signal is detected by using a shift is measured by the run length, and the average of such points is known as the ARL. The ARL can be classified as in-control ARL (denoted as ARL_0) and OOC ARL (denoted as ARL_1). An efficient chart has the smallest ARL_1 .

This article aims to present a monitoring method for upward (downward) shifts using truncated gamma distribution for time-between-events. To this end, a one-sided

EWMA is introduced to study various shifts in the scale parameter of the truncated gamma distribution. “We take an interest in one-sided TBE charts because of their significance in practical applications. The reason for considering the gamma distribution is its practical use in reliability analysis. This distribution is a generalized form of the exponential distribution. Furthermore, if the shape parameter is greater than one, the hazard rate also increases, while decreasing when the shape parameter is less than one”.

If the response variable distribution is skewed and normal distribution is assumed to develop a monitoring strategy, then the resulting charting technique will either signal a shift in the process when there is none or it will fail to detect any shift in the manufacturing process. Lucas [1] and Vardeman and Ray [2] were “the first to propose the control chart methodology based on monitoring the TBE concept. Many problems arise when a traditional control chart is used in a high-quality process monitoring and to circumvent these problems, the TBE charts are used. A TBE-type control chart is commonly developed to monitor the inter-arrival time of nonconforming items. For the TBE data, it is assumed that they follow one of the skewed distributions. As a result of the skewed nature of data, exponential distribution may or may not be sufficient to describe it appropriately. To this end, we use a truncated gamma distribution rather than an exponential distribution. The truncated gamma distribution is a conditional distribution that results from restricting the domain of the ordinary gamma distribution and it is useful to model TBES above a threshold which may occur in applications, e.g., time between a system failure is recorded if it is above one minute, etc. The gamma distribution is a generalized form of the exponential distribution. This distribution is positively skewed and contains positive values only and having shape and scale parameters. The shape of the distribution depends on the shape parameter and it becomes an exponential distribution when it is equal to one”.

Many authors focused on attribute control charts, such as Joekes and Barbosa [3], Wu and Wang [4], De Araújo Rodrigues et al. [5], and Wu et al. [6]. Woodall [7] presented a detailed review of attribute control charts. Contrary to this, many scholars have recently concentrated on the TBE charts because these charts are efficient in detecting process shifts and are competent in high-quality processes. A one-sided exponential EWMA control chart is used by Xie et al. [8], which was first developed by Gan [9]. Crowder and Hamilton [10] designed a one-sided EWMA technique for monitoring the standard deviation of a process. Shu et al. [11] proposed an improved one-sided EWMA (IEWMA) control chart to monitor the rapid detection of upward or downward changes in the process mean. Gan [12] designed a one-sided EWMA control technique and evaluated its ARL performance. Furthermore, they compared the proposal to the one-sided CUSUM control chart. We refer to Ali et al. [13] for a comprehensive overview of the TBE charts in discrete and continuous scenarios.

Kumar et al. [14] proposed a t_r -chart to monitor the TBE based on probability limit to improve the sensitivity and ability for small to moderate changes. Alevizakos and Koukouvinos [15] “proposed a new two-sided TBE control chart for monitoring low-rate of occurrences and showed that the chart performs better than the t_r , ARL-unbiased gamma, generally weighted moving averages TBE (GWMA-TBE) and double EWMA TBE (DEWMA-TBE) charts in detecting very small to steady downward shifts as well as small upward shifts in few situations”.

Qu et al. [16] introduced a new charting scheme named the two-sided TBE cumulative sum (CUSUM) chart for monitoring a decrease in the time interval T and an increase in the time interval T in a process. The developed control chart is known as the weighted cumulative sums (WCUSUM) chart. In “high-quality manufacturing processes, the TBE follows an exponential distribution. A one-sided DEWMA control chart is considered in Alevizakos and Koukouvinos [17] to detect downward mean shifts in a process.” Hu et al. [18] proposed an adaptive EWMA (AEWMA) control chart for analyzing and monitoring the TBE data. The run length properties of the AEWMA, DEWMA, and REWMA are compared by the Markov Chain approach [8]. Many other authors, such as Rahali et al. [19,20], Shah et al. [21], Saghir et al. [22], Sanusi et al. [23], Yang et al. [24], Chakraborty et al. [25],

Rao [26], Wu et al. [27], and Aslam and Jun [28], discussed the control chart for the TBE based on skewed distributions.

For the estimation of unknown parameters, Chen and Gui [29] “used an adaptive progressive type-II censoring model to estimate unknown parameters of a truncated normal distribution”. Gul et al. [30] developed a truncated model called Weibull-truncated exponential distribution. The unknown parameters of the proposed model are calculated by applying the maximum likelihood estimation (MLE) method. Saghir et al. [22] proposed the modified EWMA control chart based on a transformation scheme for monitoring gamma distributed variables and compared it to competitive charting techniques [31,32]. Rizzo and Di Bucchianico [33] studied the generalized likelihood ratio based gamma chart for TBE data that can be modeled by a Poisson process and compared its performance to its traditional competitors. Noor et al. [34] proposed the Bayesian TBE EWMA chart using exponential and transformed exponential distributions. Sarwar et al. [35] proposed the adaptive EWMA chart to monitor the Weibull process. Ali [36] proposed predictive Bayesian charts using exponential distribution for TBE.

The rest of the article is organized as follows. Section 2 introduces the gamma distribution and describes a one-sided EWMA control chart for both, the known and estimated parameters. Section 3 discusses run length properties, while a real data application is discussed in Section 4. Section 5 contains some concluding remarks and future work.

2. Control Chart for Gamma Distribution

The “gamma distribution is a legitimate extension of the exponential distribution that is used to model the sum of inter-arrival times before the ν th occurrence in a homogeneous Poisson process. That is, the gamma distribution is the sum of the exponential distribution. Let $T_1, T_2, T_3, \dots, T_\nu$ denote the time between two consecutive occurrences of events in a homogeneous Poisson process with rate parameter $1/\alpha$, where $\alpha > 0$, and the sum of inter-arrival times is represented by Y , that is, $Y = \sum_{i=1}^{\nu} T_i$. The TBE random variable Y_t follows a gamma distribution with shape parameter $\nu > 0$ and scale parameter $\alpha > 0$, i.e., $Y_t \sim \Gamma(\nu, \alpha)$. Then, the probability distribution function (PDF) of Y is defined as

$$f(y) = \frac{1}{\alpha^\nu \Gamma(\nu)} y^{(\nu-1)} \exp\left(-\frac{y}{\alpha}\right), \quad y > 0 \quad (1)$$

and the corresponding cumulative density function (CDF) is

$$F(y) = \frac{1}{\Gamma(\nu)} \Gamma\left(\nu, \frac{y}{\alpha}\right) \quad (2)$$

where $\Gamma(\nu, \frac{y}{\alpha})$ is the lower incomplete gamma function. The mean and variance of the gamma distribution are $E(Y) = \mu = \nu\alpha$ and $Var(Y) = \nu\alpha^2$, respectively “.

2.1. The Proposed One-Sided EWMA TBE Control Chart to Monitor Changes in the Process Mean

The EWMA statistic is extensively used for small shift detection in a process to monitor qualitative or quantitative events. The one-sided EWMA statistic is used when shifts are desired to detect in a specific direction.

“To present the design structure of a one-sided EMWA scheme for truncated gamma distribution, the ordinary EWMA scheme needs to be presented first. The traditional EWMA statistic is defined as

$$Q_t = \lambda_s Y_t + (1 - \lambda_s) Q_{t-1} \quad (3)$$

where $\lambda_s \in (0, 1]$ is the smoothing parameter. Practically, we take the initial value of EWMA statistic $Q_0 = 1$ for an automatic comparison purpose. Traditionally, a small value of λ_s is considered to be appropriate for detecting small changes or shifts, whereas a large value is suitable for detecting large shifts. In practice, $\lambda_s \in [0.05, 0.25]$ is considered to detect small to moderate size shifts in the process” [37].

2.2. The Proposed Charting Scheme with Known Parameters

The “design of the proposed one-sided EWMA TBE scheme is simplified by considering the scaled TBE random variable as follows.

$$U_t = \frac{Y_t}{\alpha_0} \tag{4}$$

where α_0 represents a known in-control value of the scale parameter. Then, a scaled value of the TBE random variable is defined as

$$U_t = \frac{\alpha}{\alpha_0} \times \frac{Y_t}{\alpha} = \delta \times V_t \tag{5}$$

where δ is a constant value that denotes a shift in the pre-defined IC scale parameter α_0 and V_t is a random variable, which represents the scaled TBE values and is a standard gamma distributed random variable with mean one. Furthermore, the process is assumed to start at point $t = 0$, the IC parameter is assumed to be α_0 . When $\alpha = \alpha_0$, the process is considered to be stable or in-control (IC). If $\alpha = \delta\alpha_0$ ($\delta \neq 1$), the process is considered to be out-of-control(OOC). The state where $\delta > 1$ or $0 < \delta < 1$, represents that an increase or decrease in the pre-defined process parameter α_0 and the special case $\delta = 1$ corresponds to the in-control state “.

2.3. The Proposed Scheme with Estimated Parameter

This section “discusses the estimated parameter one-sided TBE EWMA scheme as previously we discussed the chart based on the assumption that the scale parameter α_0 of the gamma distribution is known. To estimate the pre-defined scale parameter α_0 using n IC TBE observations denoted as $Y'_1, Y'_2, Y'_3, \dots, Y'_n$ collected in the Phase-I, the maximum likelihood estimator of α_0 is defined as

$$\hat{\alpha}_0 = \frac{1}{n} \sum_{l=1}^n Y'_l \tag{6}$$

By replacing $\hat{\alpha}_0$ in (4), the estimated TBE random variable \hat{U}_t is obtained, which can be written as

$$\hat{U}_t = \frac{Y_t}{\hat{\alpha}_0} \tag{7}$$

and the estimated TBE random variable \hat{U}_t is written as

$$\hat{U}_t = \frac{\alpha_0}{\hat{\alpha}_0} \times \frac{\alpha}{\alpha_0} \times \frac{Y_t}{\alpha} = W \times \delta \times V_t \tag{8}$$

where $W = \frac{\alpha_0}{\hat{\alpha}_0}$ denotes the ratio of the known in-control scale parameter α_0 to its estimator $\hat{\alpha}_0$, $\delta = \frac{\alpha}{\alpha_0}$ denote the shifts level and $V_t = \frac{Y_t}{\alpha}$ ”.

2.4. Design Structure Using a Truncated Method

The truncation method is used to acquire lower or upper values from the target or threshold. To detect the upper-sided shifts in the process mean, “the upper-sided TBE EWMA chart is adopted with a truncation method. The basic principle behind the proposed truncation approach is to acquire the TBE observations Y_t below or above the pre-defined IC mean. The truncation based upper-sided TBE EWMA control chart can be obtained by employing the upper-truncated TBE random variable, which is given as follows

$$Y_t^+ = \max(\alpha_0, Y_t) \tag{9}$$

For the scaled random variable U_t , the upper-truncated TBE random variable is defined as

$$U_t^+ = \max(1, U_t) \tag{10}$$

Let U_t be a gamma random variable with scale parameter $\alpha = 1$. The PDF of U_t is

$$f_{U_t}(u) = \frac{1}{\Gamma(\nu)} u^{\nu-1} e^{-u} \tag{11}$$

and the CDF is given as

$$F_{U_t}(u) = \frac{\Gamma(\nu, u)}{\Gamma(\nu)} \tag{12}$$

where $\Gamma(\nu, u)$ is the incomplete gamma density function. Now, we define $U_t^+ = \max(1, U_t)$ to compute the mean and variance assuming $\delta = 1$. The PDF $f_{U_t^+}(u)$ of U_t^+ is defined on $[1, \infty)$ given as

$$f_{U_t^+}(u) = F_{U_t}(1) \times I_{u=1} + f_{U_t}(u) \times I_{u>1} = \frac{\Gamma(\nu, 1)}{\Gamma(\nu)} \times I_{u=1} + \frac{1}{\Gamma(\nu)} u^{\nu-1} e^{-u} \times I_{u>1} \tag{13}$$

where $I(\cdot)$ represents the indicator function, which is equivalent to one if the condition is met, otherwise zero. Moreover, the upper-truncated TBE scaled random variable U_t^+ can be simplified further and written as

$$Q_t^+ = U_t^+$$

and the upper-sided EWMA charting statistics S_t^+ is written as

$$S_t^+ = \lambda_s Q_t^+ + (1 - \lambda_s) S_{t-1}^+ \tag{14}$$

where λ_s denotes the smoothing constant and $S_0^+ = \mu_0 = E(Q_t^+)$. The upper-sided EWMA control charting scheme shows an OOC signal when $S_t^+ > G^+$, where G^+ is the upper control limit of the proposed EWMA TBE chart”.

Due “to the estimation of the scale parameter α_0 , the upper-truncated TBE random variable \hat{U}_t^+ is written as

$$\hat{U}_t^+ = \max(1, \hat{U}_t) \tag{15}$$

and to analyze the design properly, the estimated scaling of the proposed chart is given as

$$\hat{Q}_t^+ = \hat{U}_t^+$$

Finally, the corresponding upper-sided EWMA \hat{S}_t^+ with the estimated parameter is stated as

$$\hat{S}_t^+ = \lambda_s \hat{Q}_t^+ + (1 - \lambda_s) \hat{S}_{t-1}^+ \tag{16}$$

where the starting value at time $t = 0$ is $S_0^+ = \mu_0 = E(\hat{Q}_t^+)$. For early detection of an upward shifts, the upper-sided EWMA chart records an OOC signal when $\hat{S}_t^+ > \hat{G}^+$ with the estimated parameter”.

Similarly, to detect the lower-sided shifts, “we use a lower-sided TBE EWMA chart. The TBE random variable based on the lower-truncation method can be written as

$$Y_t^- = \min(\alpha_0, Y_t) \tag{17}$$

where α_0 is the IC known scale parameter. The lower truncated TBE random variable U_t^- is defined as

$$U_t^- = \min(1, U_t) \tag{18}$$

where the PDF and CDF truncated TBE random variable U_t^- are given in Equations (11) and (12), respectively. Considering $U_t^- = \min(1, U_t)$, the PDF $f_{U_t^-}(u)$ is defined on $[0, 1]$ and is equivalent to

$$f_{U_t^-}(u) = f_{U_t}(u) \times I_{0 \leq u < 1} + (1 - F_{U_t}(1)) \times I_{u=1} = \frac{1}{\Gamma(\nu)} u^{\nu-1} e^{-u} \times I_{0 \leq u < 1} + \left(1 - \frac{\Gamma(\nu, 1)}{\Gamma(\nu)}\right) \times I_{u=1} \tag{19}$$

The simplified form of the lower scaled random variable based on truncation U_t^- can be written as

$$Q_t^- = U_t^-$$

Finally, the lower-sided EWMA charting statistic is defined as

$$S_t^- = \lambda_s Q_t^- + (1 - \lambda_s) S_t^- \quad (20)$$

where $S_0^- = \mu_0 = E(Q_t^-)$. The lower-sided TBE EWMA issues an OOC signal when $S_0^- < G^-$, where G^- is the lower control limit of the chart."

For "the estimated parameter case, the lower truncated TBE random variable \hat{U}_t^- is defined as

$$\hat{U}_t^- = \min(1, \hat{U}_t) \quad (21)$$

and the charting statistic is

$$\hat{S}_t^- = \lambda_s \hat{Q}_t^- + (1 - \lambda_s) \hat{S}_{t-1}^- \quad (22)$$

The starting value is $\hat{S}_0^- = \mu_0 = E(\hat{Q}_t^-)$. The lower-sided EWMA is constructed for detecting a decreasing shift in the production process mean".

Remark 1. It is a challenging to obtain the expression for $f_{U_t^+}(u)$ and $f_{U_t^-}(u)$ given in Equations (13) and (19) explicitly to compute the mean and variance; therefore, these can be computed numerically as the truncated gamma distribution can be generated in R [38].

The monitoring statistic for the upper truncated TBE EWMA chart for both the known and estimated parameters given in Equations (14) and (16), respectively, is real and positive number. The G (UCL) is computed as

$$G = \mu_0 \pm L \sqrt{\frac{\lambda_s}{2 - \lambda_s} \sigma_0} \quad (23)$$

where μ_0 and σ_0 are the in-control mean and variance, which are computed from the truncated gamma distribution numerically. The L is the constant factor that controls the width of the control limit.

2.5. UCL and ARL Computation Algorithm Using Simulation

The following steps are used to calculate the UCL and run length characteristics.

1. Choose the value of λ_s (smoothing parameter), the constant multiplier (L), and a sample size (n).
2. Generate the data from the truncated gamma distribution with IC parameters.
3. Repeat Step 2 W times (say 10,000). Each time compute the mean and standard deviation of the data generated in Step 2.
4. Take the average of all W times means and standard deviations. Then, compute the values of UCLs using Equation (23) for known and estimated cases to achieve the desired value of ARL_0 , e.g., 200, 370, and 500. Otherwise, revise the value of L . The following steps are adopted to compute ARL_1 .
5. Initialize $S_0 = \mu_0$, where μ_0 is equal to the IC average.
6. Introduce a shift in the scale parameter, generate data, and calculate the monitoring statistic.
7. Record the run length, a point where the monitoring statistic crosses the UCL.
8. Repeat Steps 6–7 of algorithm W times (say 10,000) with a shifted parameter, and then compute the OOC ARL_1 and $SDRL_1$ values by computing the mean and standard deviation of the recorded run length vector.

Remark 2. The same steps are used to construct the lower-truncated control chart, which is given in Equations (20) and (22).

2.6. The Existing One-Sided Gamma EWMA Chart

Gan [9] introduced the idea to use two separate one-sided exponential EWMA control charts rather than a two-sided EWMA scheme with a reflecting boundary. The charting scheme has been demonstrated to be ARL-unbiased. Likewise, two one-sided gamma EWMA charts are suggested. In the case of high-quality production processes, this control chart is used to monitor either increase or decrease in the mean of the production process.

The existing upper-sided EWMA (considered as U-EWMA) chart for the gamma TBE data is constructed only to detect an increase in the mean. The control charting statistic Z_t of the upper-sided gamma TBE chart is written as follows:

$$z_t = \max(E, \lambda_z U_t + (1 - \lambda_z)z_{t-1}) \quad (24)$$

where E represents a reflecting boundary of the upper-sided gamma EWMA chart. Here, the reflecting boundary is equal to the mean $E = \nu\theta_0$, where ν is the shape parameter and θ_0 is the IC scale parameter. The $\lambda_z \in (0, 1]$ is a weighting parameter of the upper-sided gamma scheme. An OOC signal is emitted when z_t surpasses the upper control limit g_z .

Similarly, the lower-sided (written as the L-EWMA) chart for gamma TBE data is constructed to detect a decrease in the mean. The control charting statistics z_t of the lower-sided gamma EMWA scheme is defined as

$$z_t = \min(F, \lambda_z U_t + (1 - \lambda_z)z_{t-1}) \quad (25)$$

where F denotes a lower reflecting boundary of the control chart that is equal to $F = \nu\theta_0$, and $\lambda_z \in (0, 1]$ represents a smoothing constant of the existing lower-sided gamma EWMA scheme. The scheme gives an OOC signal when z_t is less than the lower control limit g_z .

The Monte Carlo simulation method is used for evaluating the ARL performance of the existing as well as of proposed one-sided EWMA control charts based on truncated gamma distribution. Furthermore, the proposed one-sided EWMA TBE chart is also discussed for the known and estimated parameter and compared with the existing one-sided gamma EWMA chart. With the same ARL_0 , a charting scheme that generates smaller ARL_1 values is deemed more sensitive for a fixed shift δ .

3. Run Length Properties of the Proposed Chart

This study considers run length that is commonly used to assess the performance of a control chart, including the ARL, the standard deviation of run length (SDRL), and the median run length (MRL). Due to the space limitation, only two characteristics—ARL and SDRL—are presented here. The ARL is the most effective technique to evaluate the performance of a control scheme and accesses its sensitivity against shifts of different magnitudes. The ARL is defined as the average number of observations or points that must be plotted against a fixed shift on a control chart before a sample indicates an OOC signal. The ARL is classified in two forms: ARL_0 and ARL_1 . For an IC process, the ARL_0 value should be large to minimize the false-alarm rate. On the other hand, when the process is in the OOC condition, the ARL_1 value should be as small as possible to detect a process shift quickly. Since the distribution of the ARL is skewed and not geometric in the case of the EWMA chart, one should investigate its SDRL as well. Therefore, a comprehensive analysis of the control limits and run length characteristics, such as the ARL and SDRL, are given in Tables 1–5, corresponding to the upper case, and in Tables 6–10 for the lower-sided chart.

3.1. Performance Analysis under Upward Shifts

In “order to assess the ARL and SDRL performances of the proposed upper-sided TBE EWMA scheme, the control limits G^+ and \hat{G}^+ with known and estimated parameters are presented in Tables 1–3, respectively, for the desired IC $ARL_0 \in \{200, 370, 500\}$ and different values of $n \in \{10, 30, 50, 100, 200, 300, 350, +\infty\}$ when the smoothing constant $\lambda_s \in \{0.05, 0.07, 0.10, 0.20, 0.30, 0.50, 0.70, 0.90\}$. It is notable that in the known parameter case, $n = +\infty$ is considered, which means a very large sample size. The results in Tables 1–3 indicate that the control limit G^+ of the proposed upper-sided scheme increases when λ_s increase. For example, in Table 1 with $\nu = 0.5$ and $n = 10$, the upper control limit value

increased from 2.0933 to 5.2624 as λ_s increases from 0.05 to 0.90. Moreover, the control limit g_z and \hat{g}_z for known and estimated parameters are also listed in Tables 1–3, respectively. For a specified value of λ_s and ARL_0 , the \hat{G}^+ value of the proposed upper-sided TBE EWMA with estimated parameters increases or decreases and it becomes closer to the value of the known parameter case as n increases. This indicates that the impact of the estimated parameter on the performance of the proposed charting scheme is significant when the number of the TBE observations is small in Phase I”.

The “ ARL (\widehat{ARL}) and $SDRL$ (\widehat{SDRL}) values of the proposed upper-sided TBE EWMA with known (estimated) parameters are obtained by the Monte Carlo simulation method. For the known parameter case, the ARL_1 and $SDRL_1$ values with the desired $ARL_0 = 370$ are listed in Table 4 for the proposed and existing upper-sided chart, respectively. Notice that a small value of λ_s is more sensitive to small shifts in the process and vice versa. For instance, in Table 4, as λ_s increases from 0.05 to 0.90, the ARL_1 value of the proposed chart also increases from 53.62 to 105.74 with $\delta = 1.3$. The ARL_1 values decreases from 2.94 to 2.82 when $\delta = 8$. For the known parameter case, consider $\lambda_s = 0.07$ and the upward mean shift $\delta = 1.1$, the ARL_1 ($SDRL_1$) value of the proposed chart upper-sided chart is 159.51 (154.49). For the existing upper-sided gamma EWMA chart, the ARL_1 ($SDRL_1$) value is 193.28 (185.06). Similarly, for $\lambda_s = 0.30$ and the upward shift $\delta = 2$, the ARL_1 ($SDRL_1$) value for the proposed and existing control charts are 17.26 (15.77) and 23.69 (22.6), respectively. For the estimated parameter case, Table 5 lists the \widehat{ARL}_1 (\widehat{SDRL}_1) values of the proposed and existing EWMA charts constructed using $n = 350$ and the desired $ARL_0 = 370$. For the upward shift $\delta = 3$ with $\lambda_s = 0.30$, the \widehat{ARL}_1 (\widehat{SDRL}_1) value of the proposed upper-sided scheme is 7.39 (6.16) while 9.78 (8.58) for the existing upper-sided gamma EWMA chart”. Several conclusions can be made from Tables 4 and 5. For example,

- For the same smoothing constants (i.e., $\lambda_s = \lambda_z$), the proposed upper-sided TBE EWMA scheme performs uniformly better than the existing upper-sided gamma EWMA chart for both known and estimated parameters (with $n = 350$) cases in detecting the upward mean shifts.
- For a fixed value shift δ , the performance of ARL_1 ($SDRL_1$) of the proposed and existing upper-sided EWMA scheme is different as the value of λ_s (λ_z) increases. For upward mean shift $\delta = 1.3$ with $\lambda_s = 0.05$, the ARL_1 ($SDRL_1$) values of the proposed and existing upper-sided charts are 53.62 (45.77) and 75.93 (67.89), respectively. However, when $\delta = 1.3$ and λ_s is 0.9, the ARL_1 ($SDRL_1$) values of these two charting schemes are 105.74 (104.89) and 116.93 (116.28), respectively.
- In contrast to the known parameter case, the effect of the parameter estimation on the proposed scheme is relatively small. There is a slight variation between the (ARL_1 , $SDRL_1$) and (\widehat{ARL}_1 , \widehat{SDRL}_1) values of the proposed charting TBE EWMA scheme. Contrary to this case, a disparity between the (ARL_1 , $SDRL_1$) and (\widehat{ARL}_1 , \widehat{SDRL}_1) values of the existing upper-sided gamma EWMA chart is clear, especially when the smoothing constant is small. Considering the preceding remarks, it is clear that the proposed upper-sided control chart is more resistant to the effect of parameter estimation than the existing upper-sided control chart.

3.2. Performance Analysis under Downward Shifts

Detection “of shifts and monitoring changes in a process is a crucial when the events of interest are negative. To analyze the performance of the proposed lower-sided TBE EWMA scheme for the downward mean shifts, we use a similar procedure as in the case of upward shifts. The control limits G^- and \hat{G}^- of the proposed chart lower-sided TBE EWMA charting scheme with known and estimated parameter cases are listed in Tables 6–8. From the tables, the values of the control limits G^- of the proposed lower-sided TBE EWMA chart decreases when λ_s increases. For instance, consider Table 6 with $\nu = 0.5$ and $n = 10$, the lower control limit decreases from 0.1821 to 0.0027 as λ_s increased from 0.05 to 0.90. Furthermore, the control limits g_z and \hat{g}_z of the existing lower-sided gamma EWMA chart for both known and

estimated parameters are presented in Tables 6–8, respectively for the IC values of ARL_0 . The results in Table 6 tend to be closer to the known parameter value for a given value of smoothing parameter and IC ARL_0 as n increases. Also, the estimated parameter has a large impact on the performance of the ARL with a small number of TBE observations”.

Table 1. The UCL of the upper-sided TBE EWMA and existing gamma EWMA charts with $ARL_0 = 200$, $\lambda_s(\lambda_z) \in \{0.05, 0.07, 0.1, 0.2, 0.3, 0.5, 0.7, 0.9\}$ and $n \in \{10, 30, 50, 100, 200, 300, 350, 500\}$.

| Proposed | | | | | | | | |
|-----------|------------------------|--------|--------|--------|--------|--------|--------|--------|
| n | $\lambda_s(\lambda_z)$ | | | | | | | |
| | 0.05 | 0.07 | 0.1 | 0.2 | 0.3 | 0.5 | 0.7 | 0.9 |
| 10 | 2.0933 | 2.1847 | 2.313 | 2.701 | 3.0671 | 3.791 | 4.5176 | 5.2624 |
| 30 | 2.0936 | 2.1849 | 2.3134 | 2.7026 | 3.0685 | 3.7937 | 4.5177 | 5.265 |
| 50 | 2.0941 | 2.1861 | 2.3147 | 2.7047 | 3.0715 | 3.798 | 4.5255 | 5.2715 |
| 100 | 2.0944 | 2.1862 | 2.3151 | 2.7044 | 3.0718 | 3.7973 | 4.5247 | 5.2718 |
| 200 | 2.0928 | 2.1848 | 2.3129 | 2.7016 | 3.0683 | 3.7914 | 4.5182 | 5.2644 |
| 300 | 2.0925 | 2.1845 | 2.3118 | 2.6996 | 3.0646 | 3.7851 | 4.5087 | 5.2552 |
| 350 | 2.0929 | 2.1837 | 2.3116 | 2.7005 | 3.0657 | 3.7854 | 4.5135 | 5.2549 |
| $+\infty$ | 2.0914 | 2.1848 | 2.3138 | 2.7059 | 3.0712 | 3.7887 | 4.5167 | 5.2622 |
| Existing | | | | | | | | |
| n | $\lambda_s(\lambda_z)$ | | | | | | | |
| | 0.05 | 0.07 | 0.1 | 0.2 | 0.3 | 0.5 | 0.7 | 0.9 |
| 10 | 0.7763 | 0.8597 | 0.977 | 1.3359 | 1.6734 | 2.3256 | 2.9743 | 3.6149 |
| 30 | 0.776 | 0.8599 | 0.9772 | 1.3356 | 1.6736 | 2.3256 | 2.9727 | 3.6151 |
| 50 | 0.7764 | 0.8601 | 0.9781 | 1.337 | 1.6753 | 2.3304 | 2.9779 | 3.6209 |
| 100 | 0.7769 | 0.861 | 0.9781 | 1.337 | 1.6756 | 2.3286 | 2.9739 | 3.6168 |
| 200 | 0.7764 | 0.8606 | 0.9787 | 1.3376 | 1.675 | 2.3251 | 2.9677 | 3.6078 |
| 300 | 0.7773 | 0.8624 | 0.9798 | 1.3396 | 1.6767 | 2.3285 | 2.9709 | 3.6126 |
| 350 | 0.7776 | 0.8622 | 0.9796 | 1.3391 | 1.6768 | 2.3288 | 2.9719 | 3.617 |
| $+\infty$ | 0.7779 | 0.8619 | 0.9811 | 1.3386 | 1.6766 | 2.3264 | 2.9654 | 3.6098 |

Table 2. The UCL of the upper-sided TBE EWMA and existing upper-sided gamma EWMA charts with $ARL_0 = 370$, $\lambda_s(\lambda_z) \in \{0.05, 0.07, 0.1, 0.2, 0.3, 0.5, 0.7, 0.9\}$ and $n \in \{10, 30, 50, 100, 200, 300, 350, 500\}$.

| Proposed | | | | | | | | |
|-----------|------------------------|--------|--------|--------|--------|--------|--------|--------|
| n | $\lambda_s(\lambda_z)$ | | | | | | | |
| | 0.05 | 0.07 | 0.1 | 0.2 | 0.3 | 0.5 | 0.7 | 0.9 |
| 10 | 2.1542 | 2.2592 | 2.4043 | 2.8449 | 3.2624 | 4.0857 | 4.9226 | 5.7801 |
| 30 | 2.1547 | 2.2595 | 2.4049 | 2.846 | 3.2629 | 4.0862 | 4.9236 | 5.7819 |
| 50 | 2.1549 | 2.2598 | 2.4053 | 2.8468 | 3.2636 | 4.0878 | 4.9278 | 5.7841 |
| 100 | 2.1548 | 2.2595 | 2.4049 | 2.8468 | 3.262 | 4.0861 | 4.9273 | 5.7811 |
| 200 | 2.1541 | 2.2583 | 2.4032 | 2.8457 | 3.2603 | 4.0843 | 4.9263 | 5.779 |
| 300 | 2.1538 | 2.2576 | 2.4028 | 2.8449 | 3.2592 | 4.0833 | 4.9228 | 5.7765 |
| 350 | 2.1535 | 2.2575 | 2.4026 | 2.8448 | 3.259 | 4.0832 | 4.9222 | 5.7772 |
| $+\infty$ | 2.1531 | 2.2571 | 2.4021 | 2.8431 | 3.2596 | 4.0869 | 4.9208 | 5.7796 |
| Existing | | | | | | | | |
| n | $\lambda_s(\lambda_z)$ | | | | | | | |
| | 0.05 | 0.07 | 0.1 | 0.2 | 0.3 | 0.5 | 0.7 | 0.9 |
| 10 | 0.8249 | 0.9208 | 1.0551 | 1.4663 | 1.8552 | 2.6135 | 3.364 | 4.1178 |
| 30 | 0.8481 | 0.9207 | 1.055 | 1.4664 | 1.8551 | 2.6149 | 3.3649 | 4.1179 |
| 50 | 0.825 | 0.9213 | 1.0552 | 1.4674 | 1.8567 | 2.6167 | 3.3682 | 4.123 |
| 100 | 0.8253 | 0.9214 | 1.0554 | 1.4676 | 1.8566 | 2.6156 | 3.3666 | 4.1191 |
| 200 | 0.8257 | 0.9218 | 1.0564 | 1.4703 | 1.8602 | 2.618 | 3.3702 | 4.1204 |
| 300 | 0.8258 | 0.9227 | 1.0575 | 1.4701 | 1.8582 | 2.6161 | 3.3688 | 4.1183 |
| 350 | 0.8257 | 0.9221 | 1.0571 | 1.4704 | 1.8588 | 2.6162 | 3.3686 | 4.12 |
| $+\infty$ | 0.8256 | 0.9214 | 1.0566 | 1.4685 | 1.8563 | 2.6131 | 3.3675 | 4.1193 |

Table 3. The UCL of the upper-sided TBE EWMA and existing upper-sided gamma EWMA charts with $ARL_0 = 500$, $\lambda_s(\lambda_z) \in \{0.05, 0.07, 0.1, 0.2, 0.3, 0.5, 0.7, 0.9\}$ and $n \in \{10, 30, 50, 100, 200, 300, 350, 500\}$.

| Proposed | | | | | | | | |
|-----------|------------------------|--------|--------|--------|--------|--------|--------|--------|
| n | $\lambda_s(\lambda_z)$ | | | | | | | |
| | 0.05 | 0.07 | 0.1 | 0.2 | 0.3 | 0.5 | 0.7 | 0.9 |
| 10 | 2.182 | 2.2927 | 2.4468 | 2.9127 | 3.3551 | 4.2298 | 5.1173 | 6.0301 |
| 30 | 2.1817 | 2.2924 | 2.4466 | 2.913 | 3.3553 | 4.2301 | 5.1168 | 6.0275 |
| 50 | 2.182 | 2.2926 | 2.4466 | 2.9129 | 3.3551 | 4.2306 | 5.1178 | 6.029 |
| 100 | 2.1821 | 2.2929 | 2.4462 | 2.9136 | 3.3558 | 4.2337 | 5.1204 | 6.0322 |
| 200 | 2.1816 | 2.292 | 2.4456 | 2.9129 | 3.355 | 4.2323 | 5.12 | 6.0356 |
| 300 | 2.1809 | 2.291 | 2.444 | 2.9089 | 3.3513 | 4.2281 | 5.1138 | 6.0274 |
| 350 | 2.1807 | 2.2911 | 2.4441 | 2.909 | 3.3512 | 4.2286 | 5.1158 | 6.0354 |
| $+\infty$ | 2.1814 | 2.2914 | 2.4442 | 2.9097 | 3.353 | 4.2285 | 5.1184 | 6.0333 |

| Existing | | | | | | | | |
|-----------|--------|--------|--------|--------|--------|--------|--------|--------|
| 10 | 0.848 | 0.9498 | 1.0917 | 1.5304 | 1.9451 | 2.7543 | 3.557 | 4.3608 |
| 30 | 0.8481 | 0.9501 | 1.092 | 1.5305 | 1.9451 | 2.7548 | 3.5585 | 4.3639 |
| 50 | 0.8483 | 0.9504 | 1.0927 | 1.5311 | 1.9468 | 2.7569 | 3.5604 | 4.3661 |
| 100 | 0.8487 | 0.9506 | 1.0928 | 1.5309 | 1.9453 | 2.7555 | 3.5587 | 4.3646 |
| 200 | 0.8483 | 0.9504 | 1.0928 | 1.5307 | 1.9448 | 2.7558 | 3.5602 | 4.3654 |
| 300 | 0.8489 | 0.9512 | 1.0939 | 1.5309 | 1.9458 | 2.7578 | 3.5603 | 4.369 |
| 350 | 0.8486 | 0.9507 | 1.0936 | 1.531 | 1.9464 | 2.7589 | 3.5613 | 4.3709 |
| $+\infty$ | 0.8488 | 0.9507 | 1.0932 | 1.5306 | 1.9455 | 2.7552 | 3.5625 | 4.3719 |

The “ $ARL(\widehat{ARL})$ and $SDRL(\widehat{SDRL})$ performance of the proposed lower-sided TBE EWMA scheme is evaluated for the known and estimated parameter cases. In addition, a comparison of the proposed chart lower-sided TBE EWMA scheme with the existing lower-sided gamma EWMA scheme is also listed in Table 9 for $ARL_0 = 370$. It is noticed that the proposed chart outperforms the existing chart for large shifts and we attribute this to the EWMA statistic which always increases. For the known parameter case with $\lambda_s = 0.2$ and the downward mean shift $\delta = 0.1$, the $ARL_1(SDRL_1)$ value of the proposed lower-sided TBE EWMA scheme is 8.63 (2.37). For the existing chart, the $ARL_1(SDRL_1)$ value is 8.79 (1.37). It is also noticed that with the increase in the smoothing constant values, the ARL_1 values also increase from 85.92 up to 234.17 for $\delta = 0.6$. Likewise, for $\lambda_s = 0.05$ and $\delta = 0.2$, the values of the $ARL_1(SDRL_1)$ for proposed and existing charts are 15.35 (4.54) and 15.68 (2.06), respectively. For the estimated parameter, the $ARL_1(SDRL_1)$ values are tabulated in Table 10 for the proposed and existing lower-sided control charts assuming $n = 350$ and $ARL_0 = 370$. For example, when $\delta = 0.15$ and $\lambda_s = 0.07$, $\widehat{ARL}_1(\widehat{SDRL}_1)$ value of the proposed lower-sided TBE EWMA scheme is 12.16 (2.96). However, $\widehat{ARL}_1(\widehat{SDRL}_1)$ value of the existing lower-sided gamma EWMA is 13.09 (1.51). Thus, the proposed chart with the estimation effect outperforms the existing chart for large shifts”. The results tabulated in Tables 9 and 10 can be summarized as follows:

- For known and estimated parameter cases, the proposed lower-sided TBE EWMA chart outperforms the corresponding lower-sided gamma EWMA chart with a small smoothing constant for downward mean shifts detection.
- For a fixed downward mean shift δ , the performance of $ARL_1(SDRL_1)$ of the proposed and existing charts is different and does not tend to be similar because $\lambda_s(\lambda_z)$ increases for known and estimated parameter cases. For example, with $\delta = 0.5$ and $\lambda_s = 0.07$, the $ARL_1(SDRL_1)$ values are 58.81 (46.34) and 32.21 (16.41) for the estimated and known parameter cases, respectively, and the $ARL_1(SDRL_1)$ are 192.08 (188.84) and 134.05 (131.26), respectively, using $\lambda_s = 0.9$ and $\delta = 0.5$. For the estimated parameter, when $\delta = 0.3$ and $\lambda_z = 0.5$, the ARLs are 49.59 (45.31) and 28.57 (23.47), respectively, for the known and estimated parameters cases.

- The effect of the parameter estimation on the proposed and existing schemes is relatively small. This fact indicates that the suggested lower-sided TBE EWMA chart and existing lower-sided gamma EWMA scheme are both effective at resisting the effect of parameter estimation. This conclusion may be particular to the gamma distribution and cannot be generalized.

3.3. A Graphical Comparison

A graphical comparison provides additional data descriptions and clarifies the data's essence in the mind of viewers. In this section, the proposed control charts have been compared with the existing control charts using the ARL curves. The control chart's curves have been sketched taking shifts along the x-axis and the ARL values along the y-axis, for different values of $n = 10, 50, 100$. Figures 1–6 are plotted to study the ARL performance of the upper-sided proposed existing control charts at different values of smoothing constants such as 0.05, 0.10, 0.30, and 0.50 for $ARL_0 = 200$ and $ARL_0 = 500$, receptively. The graphical depiction shows that the ARL curve of the upper-sided proposed control chart performs better than the upper-sided existing control chart. Figures 7–12 are plotted to analyze the ARL performance of the lower-sided proposed and existing control charts for different values of sample sizes and smoothing parameters as described earlier. Again, it is noticed that the lower-sided proposed control scheme performs better than the lower-sided existing control scheme for small-to-moderate shifts with small smoothing parameters.

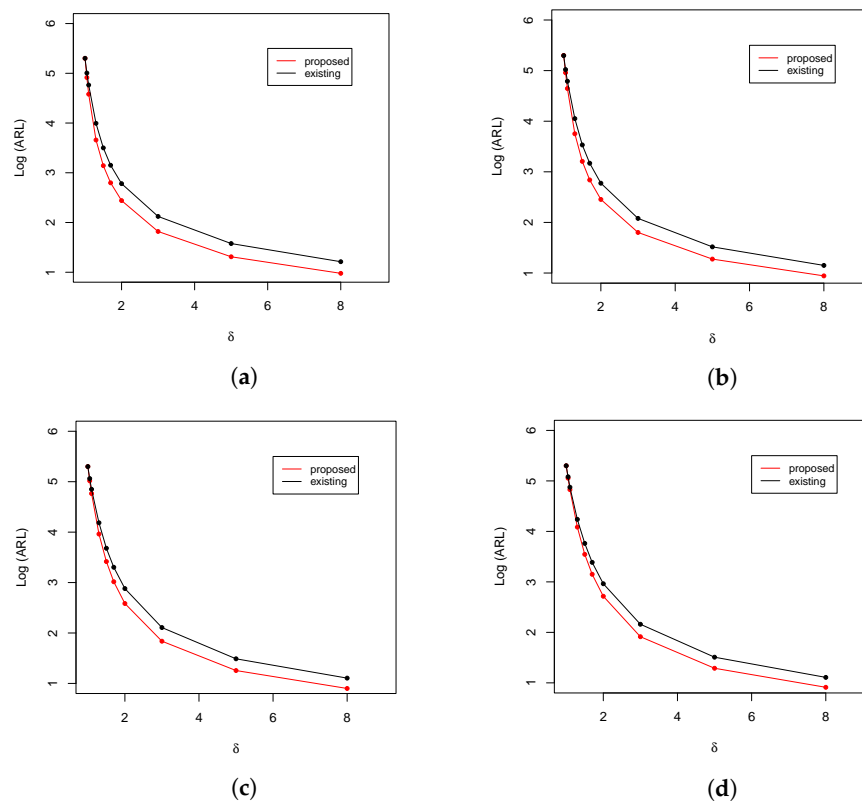


Figure 1. ARL comparison of the upper-sided control charts at $n = 10$ and $ARL_0 = 200$. (a) $\lambda = 0.05$; (b) $\lambda = 0.10$; (c) $\lambda = 0.30$; and (d) $\lambda = 0.50$.

Table 4. $ARL_1(SDRL_1)$ profiles of the upper-sided EWMA TBE and upper-sided gamma EWMA chart when $ARL_0 = 370$.

| δ | Charts | $\lambda_s (\lambda_Z)$ | 0.05 | 0.07 | 0.1 | 0.2 | 0.3 | 0.5 | 0.7 | 0.9 |
|----------|----------|-------------------------|-----------------|-----------------|-----------------|-----------------|-----------------|-----------------|-----------------|-----------------|
| | | G^+ | 2.1531 | 2.2571 | 2.4021 | 2.8431 | 3.2596 | 4.0869 | 4.9208 | 5.7796 |
| | | gz | 0.8256 | 0.9214 | 1.0566 | 1.4685 | 1.8563 | 2.6131 | 3.3675 | 4.1193 |
| 1 | Proposed | | 370.18 (365.38) | 370.3 (363.29) | 370.3 (365.05) | 370.52 (367.98) | 370.29 (363.96) | 370.21 (371.87) | 370.29 (374.89) | 370.29 (376.85) |
| | Existing | | 369.65 (369.58) | 369.65 (365.12) | 370.41 (363.49) | 370.17 (373.45) | 370.04 (374.61) | 370.33 (376.42) | 370.11 (373.59) | 369.93 (372.26) |
| 1.05 | Proposed | | 229.07 (223.64) | 237.1 (234.47) | 243.83 (240.24) | 257.33 (255.38) | 267.42 (264.37) | 279.11 (277.42) | 281.99 (283.12) | 285.28 (288.43) |
| | Existing | | 256.46 (245.83) | 259.41 (249.36) | 265.3 (255.38) | 277.03 (272.1) | 282.44 (282.58) | 288.46 (287.7) | 291.67 (291.34) | 292.21 (291.46) |
| 1.1 | Proposed | | 152.07 (144.54) | 159.51 (154.49) | 167.72 (165) | 185.87 (184.41) | 198.22 (199.29) | 215.35 (215.34) | 221.18 (220.76) | 225.9 (227.68) |
| | Existing | | 189.14 (181.44) | 193.28 (185.06) | 200.27 (193.18) | 213.05 (206.74) | 219.05 (213.91) | 227.51 (223.21) | 234.54 (233.02) | 236.22 (233.7) |
| 1.3 | Proposed | | 53.62 (45.77) | 56.75 (50.17) | 60.93 (55.5) | 72.36 (69.13) | 80.15 (79.25) | 93.15 (92.98) | 100.89 (101.45) | 105.74 (104.89) |
| | Existing | | 75.93 (67.89) | 78.82 (72.23) | 83.53 (77.75) | 93.64 (90.17) | 100.82 (97.52) | 108.73 (107.09) | 113.98 (112.92) | 116.93 (116.28) |
| 1.5 | Proposed | | 30.04 (23.57) | 30.99 (25.48) | 32.79 (28.13) | 38.18 (35.82) | 43.01 (41.15) | 50.52 (49.64) | 56.16 (55.43) | 60.15 (59.78) |
| | Existing | | 43.14 (35.94) | 44.49 (39.41) | 46.77 (43.21) | 52.62 (50.67) | 56.8 (55.39) | 62.37 (62.62) | 65.99 (65.53) | 69.19 (67.61) |
| 1.7 | Proposed | | 20.61 (15.31) | 20.99 (16.36) | 21.67 (17.67) | 24.83 (22.16) | 27.71 (25.69) | 32.71 (30.95) | 36.34 (35.35) | 39.26 (37.96) |
| | Existing | | 29.19 (23.04) | 29.72 (24.62) | 30.88 (26.88) | 34.63 (32.7) | 37.34 (36.33) | 41.64 (41.35) | 44.38 (44.46) | 46.13 (46.52) |
| 2 | Proposed | | 14.13 (9.88) | 14.11 (10.41) | 14.35 (11.19) | 15.74 (13.59) | 17.26 (15.77) | 20.02 (18.91) | 22.46 (21.49) | 24.18 (23.37) |
| | Existing | | 19.82 (14.76) | 19.84 (15.56) | 20.17 (16.82) | 22.08 (20.18) | 23.69 (22.6) | 26.23 (25.48) | 27.95 (27.46) | 28.98 (28.48) |
| 3 | Proposed | | 7.35 (4.87) | 7.17 (4.91) | 7.05 (5.05) | 7.13 (5.62) | 7.43 (6.21) | 8.25 (7.35) | 8.97 (8.27) | 9.59 (9.05) |
| | Existing | | 9.77 (6.82) | 9.53 (6.98) | 9.41 (7.22) | 9.57 (8.18) | 9.99 (8.96) | 10.72 (10.01) | 11.45 (10.85) | 11.9 (11.34) |
| 5 | Proposed | | 4.22 (2.68) | 4.1 (2.66) | 3.98 (2.68) | 3.85 (2.78) | 3.87 (2.96) | 4.03 (3.32) | 4.24 (3.63) | 4.45 (3.92) |
| | Existing | | 5.41 (3.68) | 5.21 (3.67) | 5.07 (3.72) | 4.92 (3.86) | 4.97 (4.1) | 5.2 (4.48) | 5.38 (4.83) | 5.53 (5.03) |
| 8 | Proposed | | 2.94 (1.85) | 2.87 (1.83) | 2.78 (1.81) | 2.67 (1.82) | 2.64 (1.85) | 2.66 (1.98) | 2.74 (2.12) | 2.82 (2.29) |
| | Existing | | 3.64 (2.47) | 3.51 (2.43) | 3.41 (2.4) | 3.27 (2.43) | 3.23 (2.5) | 3.28 (2.66) | 3.35 (2.78) | 3.42 (2.89) |

Table 5. $\widehat{ARL}_1(\widehat{SDRL}_1)$ profiles of the upper-sided TBE EWMA and upper-sided gamma EWMA chart when $n = 350$ and $ARL_0 = 370$.

| δ | charts | $\lambda_s (\lambda_Z)$ | 0.05 | 0.07 | 0.1 | 0.2 | 0.3 | 0.5 | 0.7 | 0.9 |
|----------|----------|-------------------------|-----------------|-----------------|-----------------|-----------------|-----------------|-----------------|-----------------|-----------------|
| | | \widehat{G}^+ | 2.1535 | 2.2575 | 2.4026 | 2.8448 | 3.259 | 4.0832 | 4.9222 | 5.7772 |
| | | \widehat{g}_Z | 0.8257 | 0.9221 | 1.0571 | 1.4704 | 1.8588 | 2.6162 | 3.3686 | 4.12 |
| 1 | Proposed | | 369.51 (367.59) | 369.58 (366.37) | 370.02 (370.38) | 369.76 (367.64) | 369.76 (365.71) | 369.81 (371.88) | 370.06 (372.16) | 370.04 (374.83) |
| | Existing | | 369.94 (364.82) | 369.64 (363.21) | 370.1 (363.25) | 370.23 (370.63) | 369.99 (371.85) | 370.04 (375.54) | 369.91 (374.79) | 370.49 (373.28) |
| 1.05 | Proposed | | 227.9 (221.74) | 234.81 (231.69) | 243.44 (240.1) | 261.63 (258.62) | 267.18 (263.79) | 277.82 (278.24) | 283.54 (286.29) | 285.48 (286.93) |
| | Existing | | 257.99 (250.66) | 264.05 (258.65) | 268.54 (262.1) | 278.69 (274.12) | 283.43 (283.21) | 288.99 (291.33) | 292.86 (294.32) | 294.74 (297.75) |
| 1.1 | Proposed | | 152.41 (145.87) | 160.99 (155.45) | 171.14 (165.78) | 191.88 (191.29) | 200.63 (200.66) | 214.29 (211.76) | 222.72 (223.06) | 226.99 (225.97) |
| | Existing | | 188.52 (181.91) | 195.61 (190.01) | 201.96 (198.28) | 214.99 (213.13) | 220.35 (219.37) | 228.44 (228.38) | 233.67 (234.56) | 237.88 (238.79) |
| 1.3 | Proposed | | 54.39 (47.47) | 57.29 (51.82) | 61.08 (55.84) | 72.62 (70.09) | 80.74 (79.71) | 92.91 (92.49) | 100.84 (99.38) | 106.62 (105.18) |
| | Existing | | 77.08 (69.67) | 80.3 (74.7) | 85.41 (82.32) | 97.3 (95.19) | 102.35 (102.2) | 110.46 (111.39) | 114.6 (115.23) | 117.9 (118.45) |
| 1.5 | Proposed | | 30.29 (23.99) | 31.27 (26.06) | 33.05 (29.04) | 39.38 (37.15) | 44.03 (43.05) | 51.33 (50.27) | 56.82 (56.24) | 59.81 (58.96) |
| | Existing | | 43.09 (36.34) | 44.38 (38.77) | 46.67 (42.43) | 53.51 (51.55) | 57.95 (56.47) | 63.76 (62.98) | 67.29 (67.21) | 69.5 (69.63) |
| 1.7 | Proposed | | 20.62 (15.38) | 20.93 (16.46) | 21.75 (17.88) | 24.95 (22.69) | 27.96 (26.57) | 32.99 (31.83) | 36.97 (36.18) | 39.89 (39.01) |
| | Existing | | 28.96 (22.76) | 29.69 (24.66) | 30.96 (27.31) | 34.65 (32.63) | 37.6 (36.22) | 41.73 (40.72) | 44.43 (43.51) | 46.19 (45.41) |
| 2 | Proposed | | 14.04 (9.82) | 14.05 (10.27) | 14.23 (11.01) | 15.58 (13.35) | 17.07 (15.46) | 20.07 (19.34) | 22.51 (22.06) | 24.43 (23.97) |
| | Existing | | 19.3 (14.27) | 19.27 (15.03) | 19.61 (16.17) | 21.41 (19.34) | 23 (21.62) | 25.49 (24.53) | 27.32 (26.5) | 28.58 (27.8) |
| 3 | Proposed | | 7.27 (4.74) | 7.12 (4.82) | 7.03 (4.95) | 7.13 (5.61) | 7.39 (6.16) | 8.17 (7.35) | 8.93 (8.24) | 9.56 (8.93) |
| | Existing | | 9.59 (6.6) | 9.35 (6.79) | 9.19 (7.01) | 9.4 (7.79) | 9.78 (8.58) | 10.52 (9.63) | 11.14 (10.54) | 11.67 (11.19) |
| 5 | Proposed | | 4.19 (2.62) | 4.07 (2.61) | 3.98 (2.63) | 3.87 (2.73) | 3.9 (2.93) | 4.04 (3.22) | 4.26 (3.53) | 4.42 (3.76) |
| | Existing | | 5.35 (3.66) | 5.17 (3.64) | 5.03 (3.65) | 4.89 (3.81) | 4.92 (4.04) | 5.09 (4.4) | 5.26 (4.68) | 5.44 (4.88) |
| 8 | Proposed | | 2.94 (1.81) | 2.86 (1.79) | 2.79 (1.78) | 2.69 (1.8) | 2.66 (1.84) | 2.7 (1.98) | 2.77 (2.12) | 2.85 (2.24) |
| | Existing | | 3.66 (2.47) | 3.53 (2.42) | 3.42 (2.39) | 3.29 (2.41) | 3.27 (2.49) | 3.29 (2.63) | 3.35 (2.77) | 3.42 (2.88) |

Table 6. The LCL of the lower-sided TBE EWMA and lower-sided gamma EWMA charts when $ARL_0 = 200$, $\lambda_s(\lambda_z) \in \{0.05, 0.07, 0.1, 0.2, 0.3, 0.5, 0.7, 0.9\}$ and $n \in \{10, 30, 50, 100, 200, 300, 350, 500\}$.

| Proposed | | | | | | | | |
|-----------|------------------------|--------|--------|--------|--------|--------|--------|--------|
| n | $\lambda_s(\lambda_z)$ | | | | | | | |
| | 0.05 | 0.07 | 0.1 | 0.2 | 0.3 | 0.5 | 0.7 | 0.9 |
| 10 | 0.1821 | 0.1634 | 0.1411 | 0.0918 | 0.062 | 0.0284 | 0.0114 | 0.0027 |
| 30 | 0.1821 | 0.1635 | 0.1411 | 0.0919 | 0.0621 | 0.0284 | 0.0115 | 0.0028 |
| 50 | 0.1822 | 0.1636 | 0.1411 | 0.092 | 0.062 | 0.0284 | 0.0114 | 0.0027 |
| 100 | 0.1823 | 0.1637 | 0.1413 | 0.0921 | 0.0623 | 0.0286 | 0.0115 | 0.0027 |
| 200 | 0.1824 | 0.1636 | 0.1412 | 0.092 | 0.0623 | 0.0284 | 0.0115 | 0.0027 |
| 300 | 0.1824 | 0.1636 | 0.1412 | 0.0919 | 0.0622 | 0.0285 | 0.0114 | 0.0027 |
| 350 | 0.1823 | 0.1635 | 0.1411 | 0.0921 | 0.0622 | 0.0284 | 0.0114 | 0.0027 |
| $+\infty$ | 0.1823 | 0.1636 | 0.1411 | 0.092 | 0.0622 | 0.0284 | 0.0115 | 0.0027 |
| Existing | | | | | | | | |
| 10 | 0.3039 | 0.2662 | 0.2234 | 0.1373 | 0.0901 | 0.0397 | 0.0157 | 0.0039 |
| 30 | 0.304 | 0.2665 | 0.2237 | 0.1376 | 0.09 | 0.0397 | 0.0157 | 0.0039 |
| 50 | 0.3044 | 0.2669 | 0.2239 | 0.1376 | 0.0902 | 0.0398 | 0.0158 | 0.0039 |
| 100 | 0.3041 | 0.2663 | 0.2234 | 0.1373 | 0.09 | 0.0395 | 0.0157 | 0.0038 |
| 200 | 0.3038 | 0.2661 | 0.2228 | 0.1369 | 0.0896 | 0.0395 | 0.0157 | 0.0038 |
| 300 | 0.3038 | 0.2662 | 0.2232 | 0.1371 | 0.0896 | 0.0397 | 0.0157 | 0.0038 |
| 350 | 0.3038 | 0.2662 | 0.2235 | 0.1376 | 0.0899 | 0.0396 | 0.0157 | 0.0038 |
| $+\infty$ | 0.3033 | 0.2665 | 0.2229 | 0.1369 | 0.0896 | 0.0397 | 0.0157 | 0.0038 |

Table 7. The LCL of the lower-sided TBE EWMA and lower-sided gamma EWMA charts with $ARL_0 = 370$, $\lambda_s(\lambda_z) \in \{0.05, 0.07, 0.1, 0.2, 0.3, 0.5, 0.7, 0.9\}$ and $n \in \{10, 30, 50, 100, 200, 300, 350, 500\}$.

| Proposed | | | | | | | | |
|-----------|------------------------|--------|--------|--------|--------|--------|--------|--------|
| n | $\lambda_s(\lambda_z)$ | | | | | | | |
| | 0.05 | 0.07 | 0.1 | 0.2 | 0.3 | 0.5 | 0.7 | 0.9 |
| 10 | 0.1705 | 0.1515 | 0.1291 | 0.0811 | 0.0532 | 0.0231 | 0.0087 | 0.0019 |
| 30 | 0.1705 | 0.1515 | 0.1291 | 0.0811 | 0.0532 | 0.0231 | 0.0087 | 0.0019 |
| 50 | 0.1705 | 0.1516 | 0.1291 | 0.081 | 0.0531 | 0.0231 | 0.0087 | 0.0019 |
| 100 | 0.1707 | 0.1516 | 0.1292 | 0.0811 | 0.0532 | 0.0231 | 0.0087 | 0.0019 |
| 200 | 0.1707 | 0.1517 | 0.1293 | 0.0814 | 0.0534 | 0.0231 | 0.0087 | 0.0019 |
| 300 | 0.1707 | 0.1518 | 0.1293 | 0.0814 | 0.0534 | 0.0231 | 0.0087 | 0.0019 |
| 350 | 0.1705 | 0.1516 | 0.1291 | 0.0813 | 0.0534 | 0.0231 | 0.0087 | 0.0019 |
| $+\infty$ | 0.1703 | 0.1515 | 0.1291 | 0.0812 | 0.0534 | 0.023 | 0.0087 | 0.0019 |
| Existing | | | | | | | | |
| 10 | 0.2823 | 0.2457 | 0.2038 | 0.1211 | 0.0769 | 0.0321 | 0.012 | 0.0026 |
| 30 | 0.2833 | 0.2458 | 0.2037 | 0.1211 | 0.0769 | 0.0321 | 0.012 | 0.0026 |
| 50 | 0.2834 | 0.2459 | 0.2038 | 0.1211 | 0.077 | 0.0321 | 0.012 | 0.0026 |
| 100 | 0.2836 | 0.246 | 0.2037 | 0.1213 | 0.077 | 0.0322 | 0.012 | 0.0026 |
| 200 | 0.2831 | 0.2456 | 0.2032 | 0.1208 | 0.0768 | 0.0321 | 0.012 | 0.0026 |
| 300 | 0.2833 | 0.2455 | 0.2032 | 0.1208 | 0.0769 | 0.0321 | 0.0119 | 0.0026 |
| 350 | 0.2835 | 0.2459 | 0.2035 | 0.121 | 0.077 | 0.0322 | 0.012 | 0.0026 |
| $+\infty$ | 0.2832 | 0.2455 | 0.2035 | 0.1207 | 0.0767 | 0.0321 | 0.012 | 0.0026 |

Table 8. The LCL of the lower-sided TBE EWMA and lower-sided gamma EWMA charts with $ARL_0 = 500$, $\lambda_s(\lambda_z) \in \{0.05, 0.07, 0.1, 0.2, 0.3, 0.5, 0.7, 0.9\}$ and $n \in \{10, 30, 50, 100, 200, 300, 350, 500\}$.

| Proposed | | | | | | | | |
|-----------|------------------------|--------|--------|--------|--------|--------|--------|--------|
| n | $\lambda_s(\lambda_z)$ | | | | | | | |
| | 0.05 | 0.07 | 0.1 | 0.2 | 0.3 | 0.5 | 0.7 | 0.9 |
| 10 | 0.1655 | 0.1465 | 0.1242 | 0.0767 | 0.0495 | 0.0209 | 0.0077 | 0.0016 |
| 30 | 0.1656 | 0.1465 | 0.1242 | 0.0767 | 0.0496 | 0.0209 | 0.0077 | 0.0016 |
| 50 | 0.1655 | 0.1465 | 0.1241 | 0.0767 | 0.0496 | 0.0209 | 0.0077 | 0.0016 |
| 100 | 0.1656 | 0.1466 | 0.1243 | 0.0768 | 0.0497 | 0.0209 | 0.0077 | 0.0016 |
| 200 | 0.1657 | 0.1467 | 0.1243 | 0.0768 | 0.0497 | 0.0209 | 0.0077 | 0.0016 |
| 300 | 0.1655 | 0.1466 | 0.1241 | 0.0767 | 0.0496 | 0.0208 | 0.0077 | 0.0015 |
| 350 | 0.1654 | 0.1464 | 0.124 | 0.0766 | 0.0496 | 0.0208 | 0.0077 | 0.0015 |
| $+\infty$ | 0.1653 | 0.1463 | 0.1239 | 0.0766 | 0.0496 | 0.0209 | 0.0076 | 0.0015 |
| Existing | | | | | | | | |
| n | $\lambda_s(\lambda_z)$ | | | | | | | |
| | 0.05 | 0.07 | 0.1 | 0.2 | 0.3 | 0.5 | 0.7 | 0.9 |
| 10 | 0.2745 | 0.2369 | 0.1952 | 0.1142 | 0.0716 | 0.0292 | 0.0105 | 0.0021 |
| 30 | 0.2746 | 0.2369 | 0.1953 | 0.1142 | 0.0717 | 0.0292 | 0.0105 | 0.0021 |
| 50 | 0.2747 | 0.2371 | 0.1952 | 0.1142 | 0.0717 | 0.0292 | 0.0105 | 0.0022 |
| 100 | 0.2747 | 0.2371 | 0.1954 | 0.1142 | 0.0716 | 0.0291 | 0.0105 | 0.0021 |
| 200 | 0.2744 | 0.2368 | 0.1953 | 0.114 | 0.0715 | 0.0291 | 0.0105 | 0.0021 |
| 300 | 0.2746 | 0.2368 | 0.1953 | 0.114 | 0.0714 | 0.0291 | 0.0105 | 0.0021 |
| 350 | 0.2746 | 0.2369 | 0.1955 | 0.1142 | 0.0715 | 0.0291 | 0.0105 | 0.0021 |
| $+\infty$ | 0.2745 | 0.2369 | 0.1954 | 0.1141 | 0.0715 | 0.0291 | 0.0105 | 0.0021 |

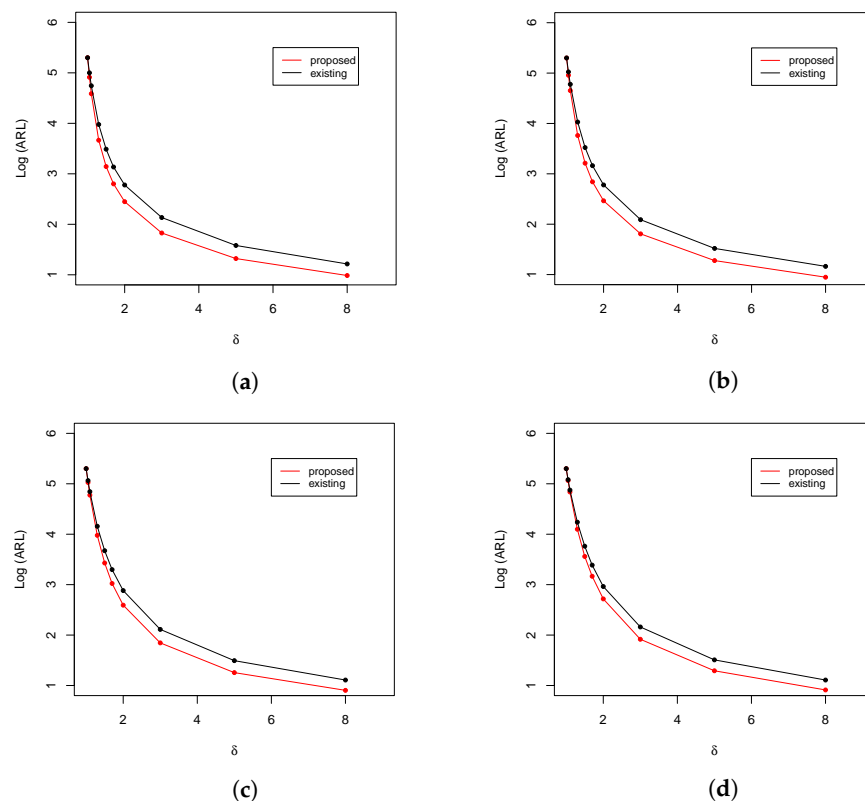


Figure 2. ARL comparison of the upper-sided control charts at $n = 50$ with $ARL_0 = 200$. (a) $\lambda = 0.05$; (b) $\lambda = 0.10$; (c) $\lambda = 0.30$; and (d) $\lambda = 0.50$.

Table 9. $ARL_1(SDRL_1)$ profiles of the lower-sided TBE EWMA and lower-sided gamma EWMA chart when $ARL_0 = 370$.

| δ | Charts | $\lambda_s (\lambda_z)$ | 0.05 | 0.07 | 0.1 | 0.2 | 0.3 | 0.5 | 0.7 | 0.9 |
|----------|----------|-------------------------|-----------------|-----------------|-----------------|-----------------|-----------------|-----------------|-----------------|-----------------|
| | | G^- | 0.1703 | 0.1515 | 0.1291 | 0.0812 | 0.0534 | 0.023 | 0.0087 | 0.0019 |
| | | g_z | 0.2832 | 0.2455 | 0.2035 | 0.1207 | 0.0767 | 0.0321 | 0.012 | 0.0026 |
| 1 | Proposed | | 370.83 (360.27) | 370.05 (359.99) | 370.11 (366.52) | 369.92 (366.92) | 370.83 (367.03) | 370.72 (372.91) | 369.96 (372.78) | 370.05 (368.35) |
| | Existing | | 369.77 (347.68) | 369.53 (348.21) | 369.97 (352.87) | 370.43 (362.27) | 370.89 (362.13) | 370.63 (364.78) | 369.95 (359.91) | 369.56 (365.87) |
| 0.8 | Proposed | | 192.33 (180.46) | 199.75 (190.28) | 209.95 (202.83) | 236.94 (235.15) | 249.87 (245.9) | 272.89 (274.07) | 289.14 (291.15) | 308.71 (303.9) |
| | Existing | | 115.03 (92.73) | 122.98 (105.36) | 132.25 (118.72) | 161.5 (151.22) | 185.69 (178.05) | 218.72 (216.23) | 242.45 (236.54) | 263.35 (260.6) |
| 0.6 | Proposed | | 85.92 (70.67) | 92.14 (79.06) | 100.49 (90.28) | 123.72 (118.93) | 142.14 (139) | 173.09 (170.68) | 201.56 (198.78) | 234.17 (229.66) |
| | Existing | | 45.44 (25.99) | 47.36 (30.37) | 50.95 (36.57) | 66.59 (56.66) | 82.2 (74.54) | 110.1 (104.44) | 138.49 (134.67) | 172.5 (171.32) |
| 0.5 | Proposed | | 55.7 (41.08) | 58.81 (46.34) | 64.39 (53.46) | 81.08 (74.62) | 96.87 (91.51) | 126.37 (123.14) | 154.62 (153.39) | 192.08 (188.84) |
| | Existing | | 32.19 (14.2) | 32.21 (16.41) | 33.33 (19.74) | 41.84 (32.3) | 52.27 (44.26) | 74.69 (69.57) | 99.22 (95.46) | 134.05 (131.26) |
| 0.4 | Proposed | | 35.84 (21.89) | 37.19 (25.03) | 39.64 (29.26) | 49.54 (41.85) | 59.59 (53.77) | 83.78 (80.2) | 110.17 (108.3) | 147.31 (145.99) |
| | Existing | | 24.08 (7.54) | 23.23 (8.55) | 23.09 (10.29) | 26.47 (17.46) | 32.42 (25.15) | 47.48 (42.11) | 67.01 (63.81) | 98.6 (97.22) |
| 0.3 | Proposed | | 23.13 (10.71) | 23.18 (11.86) | 23.88 (13.84) | 28.02 (20.44) | 33.93 (27.77) | 49.34 (45.13) | 69.35 (65.97) | 101.79 (100.16) |
| | Existing | | 19.07 (4.14) | 17.88 (4.55) | 17 (5.3) | 17.21 (8.35) | 19.81 (12.55) | 28.82 (23.65) | 42.43 (38.61) | 66.9 (63.97) |
| 0.25 | Proposed | | 18.74 (7.09) | 18.43 (7.82) | 18.46 (8.99) | 20.77 (13.55) | 24.33 (18.3) | 35.69 (31.04) | 51.6 (48.68) | 80.75 (79.02) |
| | Existing | | 17.22 (2.95) | 15.97 (3.28) | 14.91 (3.77) | 14.19 (5.74) | 15.58 (8.57) | 21.67 (16.56) | 32.43 (28.64) | 52.96 (49.75) |
| 0.2 | Proposed | | 15.35 (4.54) | 14.81 (4.98) | 14.49 (5.52) | 15.2 (8.15) | 17.38 (11.61) | 24.68 (20.15) | 36.89 (33.75) | 60.37 (58.6) |
| | Existing | | 15.68 (2.06) | 14.38 (2.23) | 13.21 (2.56) | 11.97 (3.89) | 12.32 (5.68) | 15.91 (10.74) | 23.64 (20.02) | 40.32 (37.31) |
| 0.15 | Proposed | | 12.77 (2.77) | 12.15 (2.95) | 11.61 (3.3) | 11.35 (4.68) | 12.19 (6.47) | 16.22 (11.97) | 24.06 (20.58) | 42.09 (39.34) |
| | Existing | | 14.39 (1.41) | 13.07 (1.47) | 11.84 (1.66) | 10.17 (2.45) | 9.93 (3.53) | 11.6 (6.75) | 16.56 (12.72) | 28.94 (26.26) |
| 0.1 | Proposed | | 10.82 (1.5) | 10.14 (1.57) | 9.52 (1.72) | 8.63 (2.37) | 8.63 (3.25) | 10.36 (6.06) | 14.69 (11.34) | 26.12 (23.31) |
| | Existing | | 13.3 (0.86) | 11.98 (0.89) | 10.73 (0.97) | 8.79 (1.37) | 8.13 (1.94) | 8.46 (3.74) | 10.92 (7.27) | 18.81 (16.16) |

Table 10. $\widehat{ARL}_1(\widehat{SDRL}_1)$ profiles of the lower-sided TBE EWMA and lower-sided gamma EWMA chart when $n = 350$ and $ARL_0 = 370$.

| δ | Charts | $\lambda_s (\lambda_z)$ | 0.05 | 0.07 | 0.1 | 0.2 | 0.3 | 0.5 | 0.7 | 0.9 |
|----------|----------|-------------------------|-----------------|-----------------|-----------------|-----------------|-----------------|-----------------|-----------------|-----------------|
| | | \widehat{G}^- | 0.1705 | 0.1516 | 0.1291 | 0.0813 | 0.0534 | 0.0231 | 0.0087 | 0.0019 |
| | | \widehat{g}_z | 0.2835 | 0.2459 | 0.2035 | 0.121 | 0.077 | 0.0322 | 0.012 | 0.0026 |
| 1 | Proposed | | 369.53 (357.99) | 369.61 (357.44) | 370.24 (363.72) | 369.65 (366.54) | 369.54 (365.74) | 370.13 (370.45) | 370.11 (366.29) | 370.23 (365.6) |
| | Existing | | 370.12 (348.87) | 369.87 (351.14) | 370.03 (350.69) | 370.17 (361.97) | 369.52 (360.41) | 370.49 (362.62) | 370.52 (365.6) | 370.18 (372.52) |
| 0.8 | Proposed | | 189.5 (177.51) | 197.9 (188.14) | 209.83 (201.17) | 235.39 (232.78) | 248.73 (244.94) | 272.76 (271.07) | 289.11 (288.05) | 311.26 (306.24) |
| | Existing | | 116.71 (95.38) | 125.03 (106.54) | 137 (121.38) | 164.32 (153.69) | 185.1 (175.85) | 215.21 (212.56) | 239.45 (233.06) | 263.41 (288.43) |
| 0.6 | Proposed | | 85.44 (69.79) | 91.41 (77.69) | 100.07 (88.11) | 123.03 (114.45) | 141.84 (137.23) | 172.62 (169.28) | 198.61 (196.21) | 235.71 (233.01) |
| | Existing | | 45.89 (26.21) | 47.58 (30.68) | 51.65 (37.36) | 66.44 (56.13) | 81.13 (73.01) | 110.86 (106.29) | 138.93 (133.93) | 173.08 (168.94) |
| 0.5 | Proposed | | 55.24 (40.56) | 58.46 (45.61) | 64.4 (52.93) | 81.25 (72.51) | 97.08 (89.87) | 126.16 (122.78) | 153.85 (148.97) | 191.7 (188.51) |
| | Existing | | 32.13 (13.87) | 32.13 (16.19) | 33.67 (20.14) | 42.18 (32.89) | 51.93 (44.22) | 73.21 (68.59) | 99.12 (95.11) | 133.48 (129.26) |
| 0.4 | Proposed | | 35.4 (22.27) | 36.7 (24.99) | 39.31 (29.25) | 47.7 (42.5) | 60.44 (54.65) | 83.97 (79.79) | 109.66 (105.45) | 147.95 (145.38) |
| | Existing | | 24.24 (7.76) | 23.47 (8.86) | 23.37 (10.7) | 26.6 (17.48) | 32.54 (25.47) | 47.72 (42.41) | 67.6 (63.8) | 97.81 (93.6) |
| 0.3 | Proposed | | 23.01 (10.58) | 23.05 (11.83) | 23.62 (13.87) | 27.89 (20.87) | 33.79 (27.85) | 49.59 (45.31) | 68.93 (65.34) | 103.62 (100.35) |
| | Existing | | 19.12 (4.13) | 17.92 (4.56) | 17.11 (5.39) | 17.37 (8.59) | 19.97 (12.89) | 28.57 (23.47) | 42.32 (37.82) | 66.82 (63.61) |
| 0.25 | Proposed | | 18.74 (7.16) | 18.41 (7.8) | 19.52 (9) | 20.6 (13.53) | 24.43 (18.66) | 35.7 (31.56) | 52.08 (48.47) | 81.31 (78.02) |
| | Existing | | 17.26 (2.99) | 16.01 (3.29) | 14.99 (3.8) | 14.32 (5.86) | 15.61 (8.66) | 21.74 (16.75) | 32.39 (28.45) | 53.03 (50.09) |
| 0.2 | Proposed | | 15.38 (4.57) | 14.88 (4.98) | 14.58 (5.6) | 15.34 (8.25) | 17.37 (11.63) | 24.7 (20.36) | 36.95 (33.29) | 61.05 (58.73) |
| | Existing | | 15.71 (2.11) | 14.41 (2.26) | 13.24 (2.55) | 11.99 (3.85) | 12.45 (5.82) | 16.18 (11.32) | 23.76 (19.68) | 40.86 (37.98) |
| 0.15 | Proposed | | 12.76 (2.76) | 12.16 (2.96) | 11.64 (3.29) | 11.35 (4.63) | 12.2 (6.54) | 16.4 (11.99) | 24.46 (21.34) | 52.58 (40.19) |
| | Existing | | 14.39 (1.41) | 13.09 (1.51) | 11.88 (1.66) | 10.2 (2.46) | 9.96 (3.57) | 11.78 (7) | 16.72 (12.99) | 28.86 (25.87) |
| 0.1 | Proposed | | 10.82 (1.49) | 10.15 (1.59) | 9.52 (1.7) | 8.64 (2.34) | 8.65 (3.2) | 10.37 (6.04) | 14.46 (11.26) | 26.28 (23.72) |
| | Existing | | 13.29 (0.87) | 11.97 (0.9) | 10.74 (0.97) | 8.8 (1.39) | 8.1 (1.93) | 8.45 (3.73) | 11.04 (7.47) | 18.93 (16.18) |

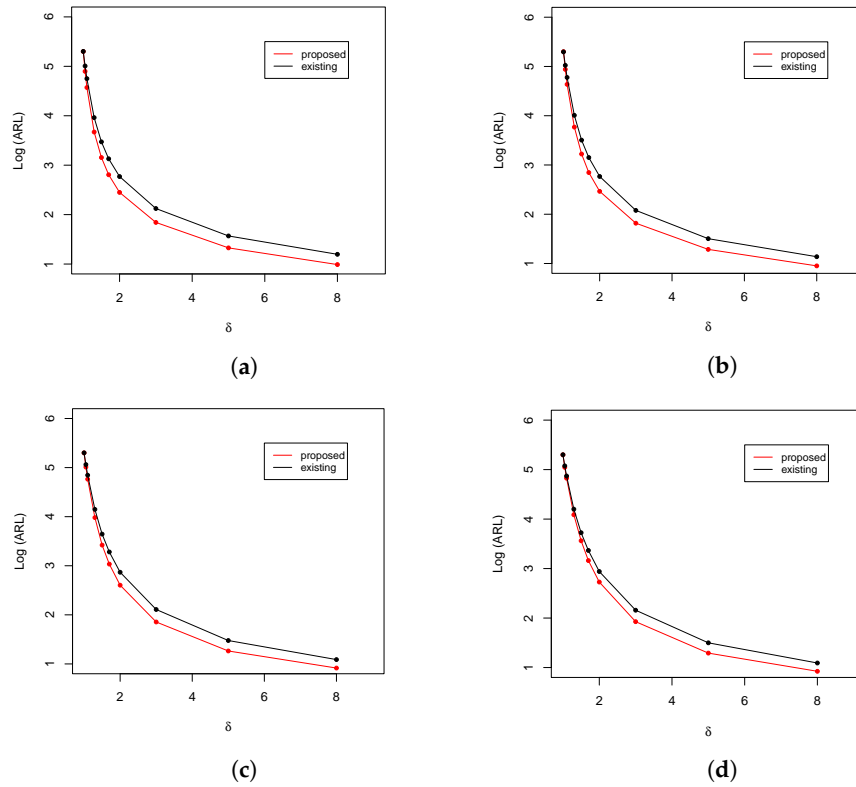


Figure 3. ARL comparison of the upper-sided control charts at $n = 100$ and $ARL_0 = 200$. (a) $\lambda = 0.05$; (b) $\lambda = 0.10$; (c) $\lambda = 0.30$; and (d) $\lambda = 0.50$.

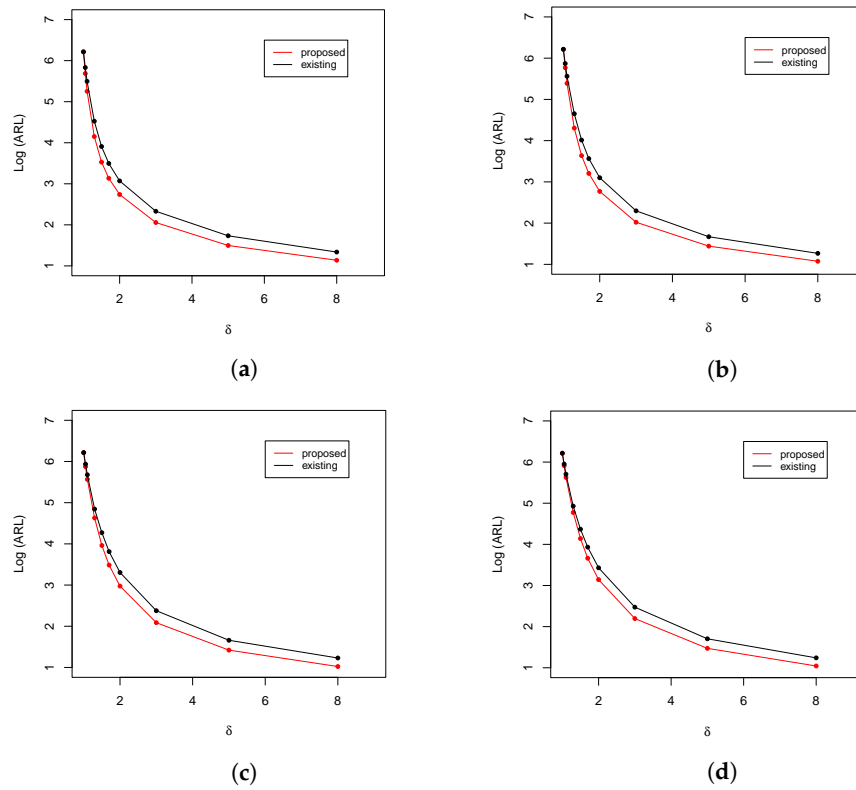


Figure 4. ARL comparison of the upper-sided control charts at $n = 10$ and $ARL_0 = 500$. (a) $\lambda = 0.05$; (b) $\lambda = 0.10$; (c) $\lambda = 0.30$; and (d) $\lambda = 0.50$.

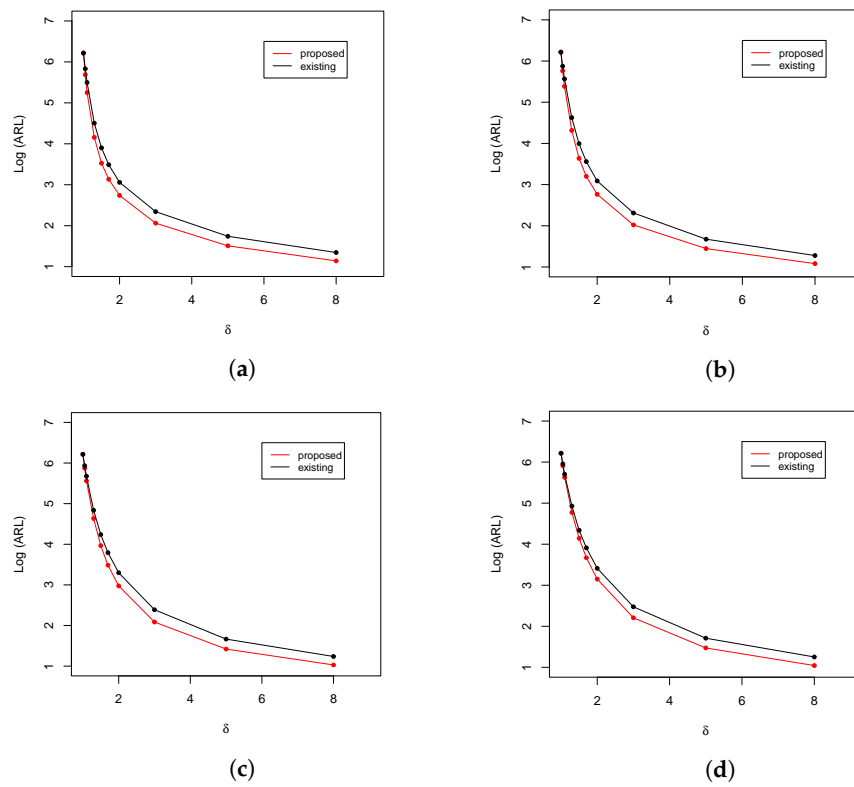


Figure 5. ARL comparison of the upper-sided control charts at $n = 50$ and $ARL_0 = 500$. (a) $\lambda = 0.05$; (b) $\lambda = 0.10$; (c) $\lambda = 0.30$; and (d) $\lambda = 0.50$.

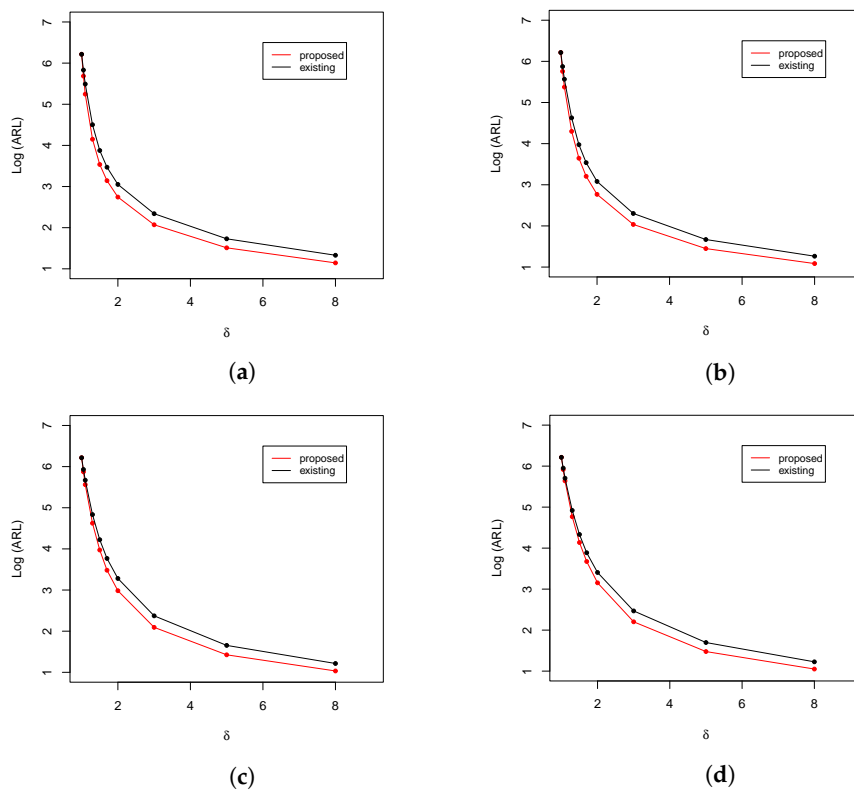


Figure 6. ARL comparison of the upper-sided control charts at $n = 100$ and $ARL_0 = 500$. (a) $\lambda = 0.05$; (b) $\lambda = 0.10$; (c) $\lambda = 0.30$; and (d) $\lambda = 0.50$.

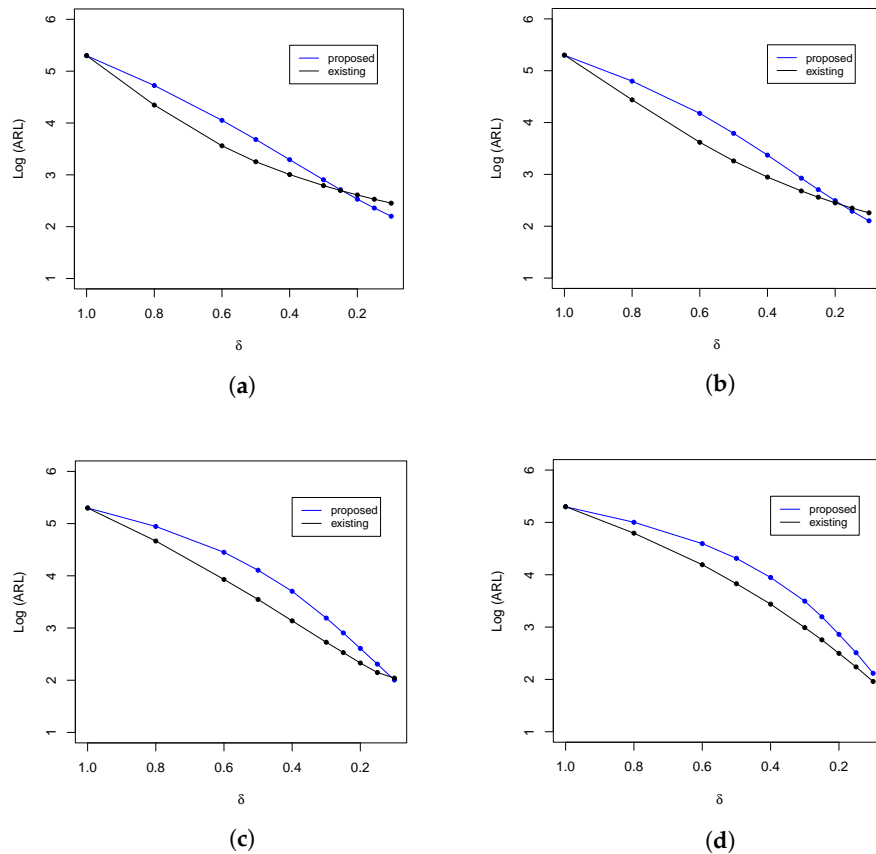


Figure 7. ARL comparison of the lower-sided control charts at $n = 10$ with $ARL_0 = 200$. (a) $\lambda = 0.05$; (b) $\lambda = 0.10$; (c) $\lambda = 0.30$; and (d) $\lambda = 0.50$.

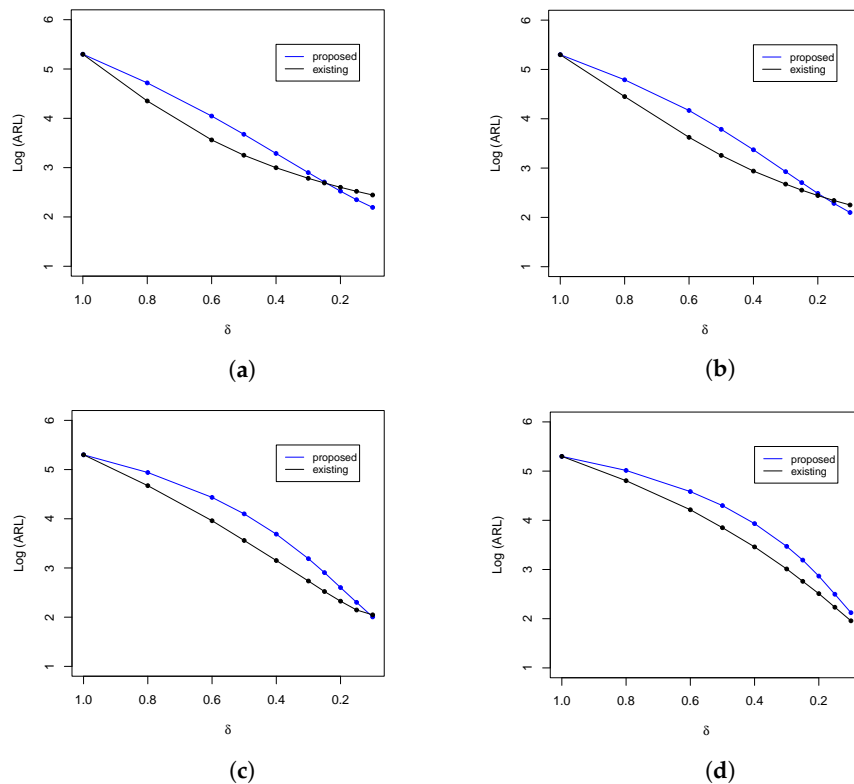


Figure 8. ARL comparison of the lower-sided control charts at $n = 50$ and $ARL_0 = 200$. (a) $\lambda = 0.05$; (b) $\lambda = 0.10$; (c) $\lambda = 0.30$; and (d) $\lambda = 0.50$.

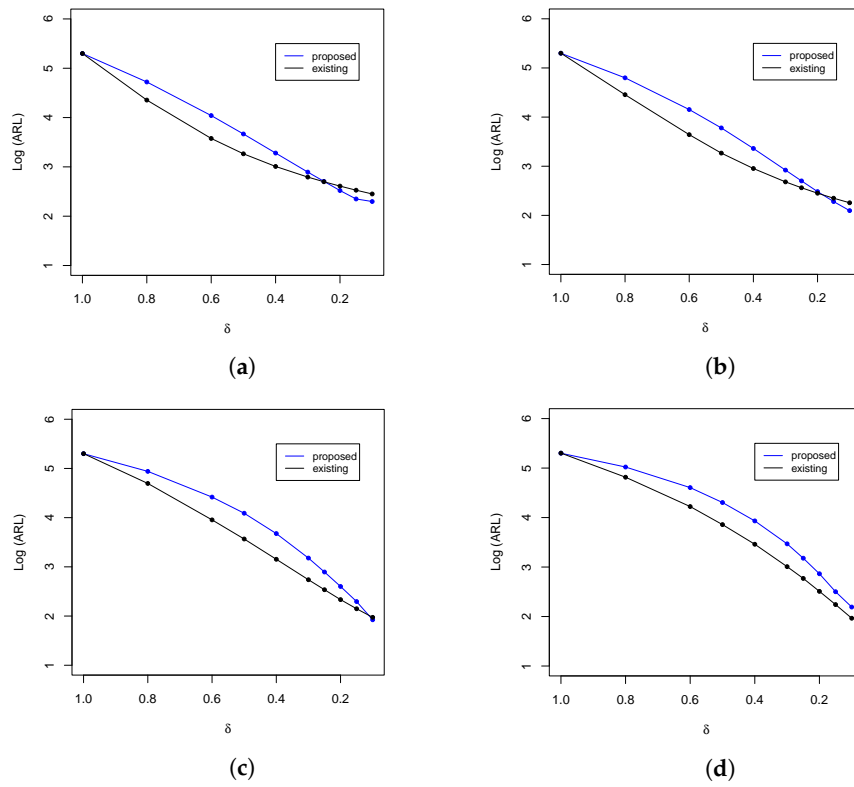


Figure 9. ARL comparison of the lower-sided control charts at $n = 100$ and $ARL_0 = 200$. (a) $\lambda = 0.05$; (b) $\lambda = 0.10$; (c) $\lambda = 0.30$; and (d) $\lambda = 0.50$.

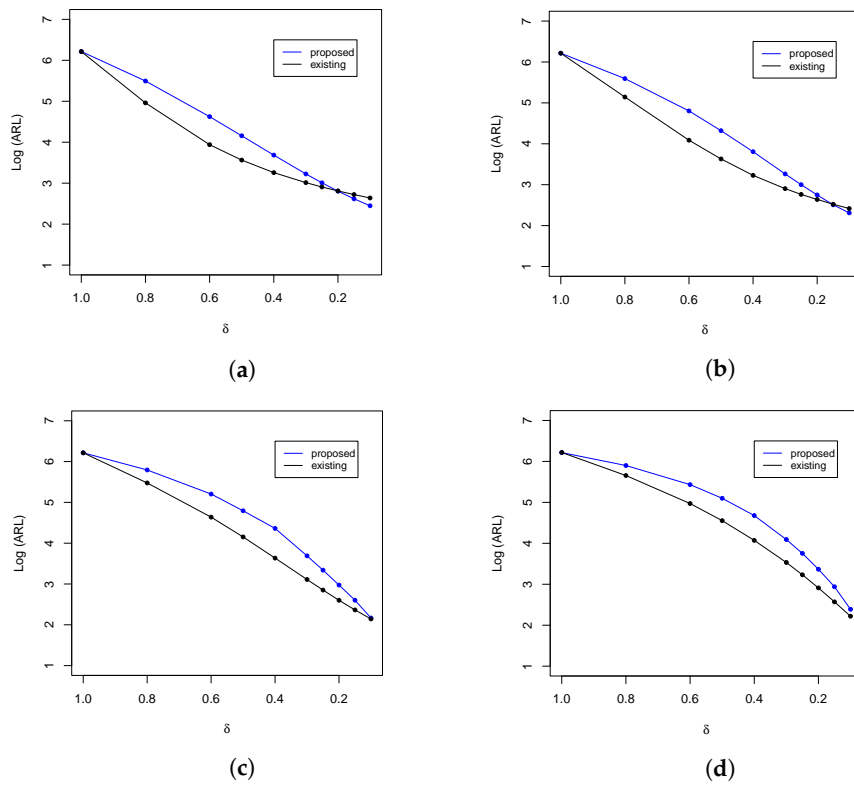


Figure 10. ARL comparison of the lower-sided control charts at $n = 10$ with $ARL_0 = 500$. (a) $\lambda = 0.05$; (b) $\lambda = 0.10$; (c) $\lambda = 0.30$; and (d) $\lambda = 0.9$.

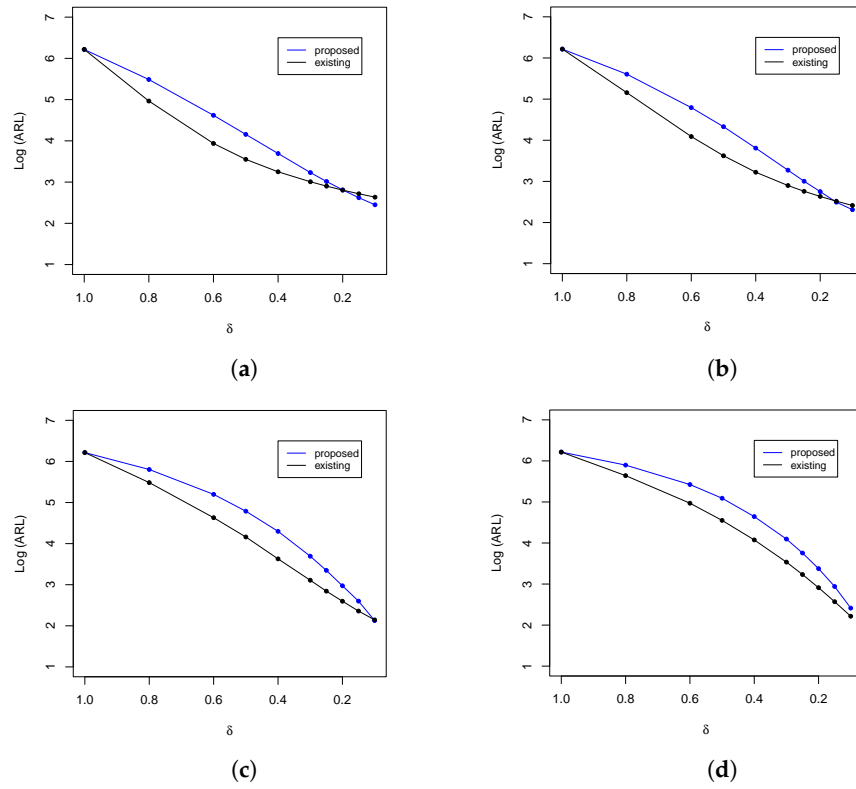


Figure 11. ARL comparison of the lower-sided control charts at $n = 50$ and $ARL_0 = 500$. (a) $\lambda = 0.05$; (b) $\lambda = 0.10$; (c) $\lambda = 0.30$; and (d) $\lambda = 0.50$.

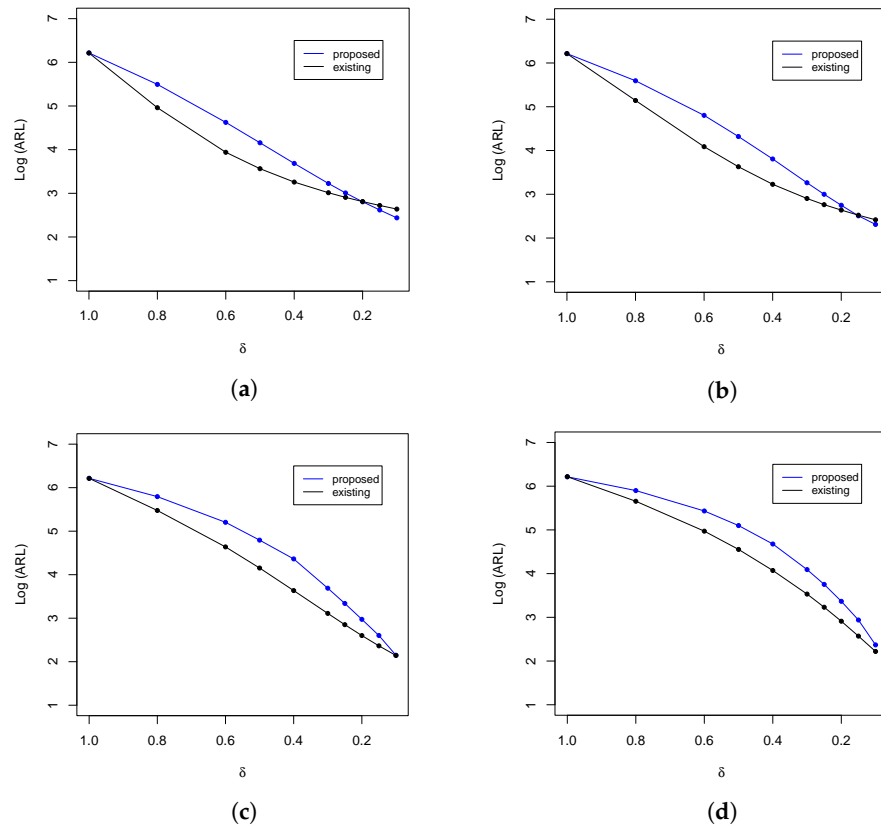


Figure 12. ARL comparison of the lower-sided control charts at $n = 100$ and $ARL_0 = 500$. (a) $\lambda = 0.05$; (b) $\lambda = 0.10$; (c) $\lambda = 0.30$; and (d) $\lambda = 0.50$.

4. A Real Data Application

In this section, the proposed methodology is implemented in a real data set. The data set consists of 16-time intervals between consecutive accidents of the F-16 aircraft of the Hellenic Air Force (HAF) and is obtained from Alevizakos and Koukouvinos [17]. The time between two aircraft accidents (T) can be regarded a crucial quality metric for monitoring reliability. The cost of the accidents necessitates that every effort is made to control the damage to preserve the HAF’s flight capability. As a critical quality attribute, the time to an accident of the F-16 aircraft supplied by Greece from 1 December 1988 to 31 December 2017 is listed in Table 11. It can be noted that the first accident occurred on 26 November 1993, i.e., 1456 days after the first acceptance of F-16. We assumed that the IC value of α_0 is 1500 (days) [17], which means that the process is in the IC state if on average an accident happened about every four years. According to Alevizakos and Koukouvinos [17], it has been proved that using the chi-square goodness of fit test, the time between accidents of the F-16 aircraft follows a gamma distribution with the shape parameter $\nu = 1$ and the scale parameter $\alpha = 615$ (i.e., $\Gamma(1615)$).

Table 11. Time between consecutive accidents of F-16 (1 December 1988–31 December 2017).

| Accidents No. | T (Days) | Accidents No. | T (Days) |
|---------------|----------|---------------|----------|
| 1 | 1456 | 9 | 499 |
| 2 | 231 | 10 | 587 |
| 3 | 691 | 11 | 561 |
| 4 | 122 | 12 | 547 |
| 5 | 718 | 13 | 448 |
| 6 | 1147 | 14 | 1561 |
| 7 | 225 | 15 | 53 |
| 8 | 706 | 16 | 280 |

To monitor the process, a lower-sided TBE EWMA chart is used. Using the Monte Carlo simulation, the control limits G^- and g_z of the lower-sided TBE EWMA and the lower-sided gamma EWMA scheme are 0.8536 and 0.6621, respectively. We set smoothing constants $\lambda_s = \lambda_z = 0.05$ with the desired $ARL_0 = 370$. The statistics S_t^- and z_t are obtained by using Equations (20) and (25) and the aforementioned design considerations. In Figure 13, the monitoring statistics are plotted against the control limits, where the red circle represent the OOC point while IC points with black dots. It is noticed that for the existing lower-sided gamma EWMA chart, there is no OOC signal, while the proposed lower-sided chart shows an OOC signal at the 16th TBE value. Hence, the proposed lower-sided TBE EWMA scheme performs better than the existing lower-sided chart in monitoring aircraft data.

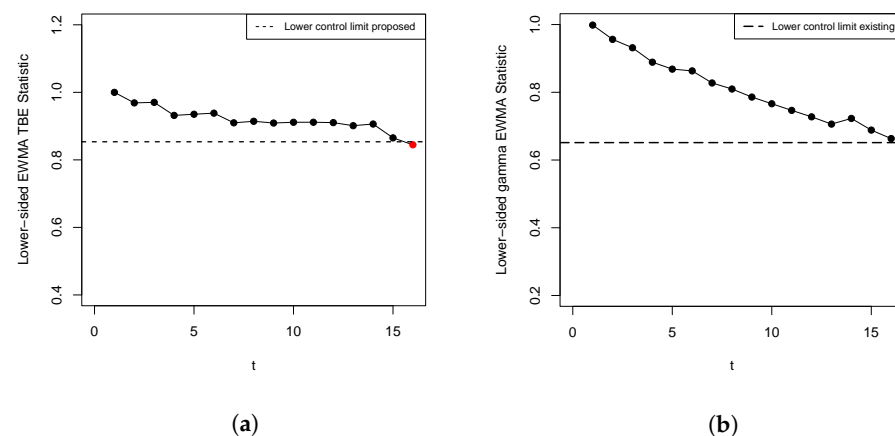


Figure 13. Lower-sided proposed and existing TBE EWMA charts. (a) Proposed chart; (b) existing chart.

5. Conclusions and Future Recommendations

There are many real-life situations where we deal with the TBE data, and numerous studies have been conducted on the TBE charts. This article introduced a one-sided memory-type control chart using a truncated gamma distribution. In particular, a one-sided TBE EWMA chart is employed for detecting upward or downward mean shifts. Besides a comprehensive simulation study, the proposed control chart is applied to a real data set. By comparing the proposed scheme with the existing chart assuming known and estimated parameter cases, it is noticed that the proposed scheme outperforms the existing chart.

The study assumed gamma distribution, which is a continuous distribution. Different types of processes may exhibit discrete data characteristics, and extending the method to these distributions could enhance its versatility. Hence, it is recommended to extend the current approach for discrete distributions like Poisson, negative binomial, and zero-inflated Poisson. The present study focussed on the EWMA chart, and it can be extended to a cumulative sum chart, which is also widely used for process monitoring. CUSUM charts are known for their sensitivity to small shifts, making them suitable for certain applications. Also, the use of a fixed smoothing constant value in the EWMA chart based on the assumption that a small value is suitable for small shifts and vice versa is not very reliable since we cannot anticipate whether the shift is large or small. To deal with this particular issue, an adaptive one-sided EWMA chart can be constructed.

Author Contributions: Conceptualization, S.R. and S.A.; methodology, S.R. and I.S.; software, S.R. and S.A.; validation, S.R., I.S. and H.H.; formal analysis, S.R. and S.A.; investigation, S.R. and S.A.; resources, I.S., H.H. and S.A.; data curation, S.A. and I.S.; writing—original draft preparation, S.R., S.A. and H.H.; writing—review and editing, S.A. and I.S.; visualization, S.R. and I.S.; supervision, S.A. and I.S.; project administration, S.A., I.S. and H.H.; and funding acquisition, H.H. All of the authors have read and agreed to the published version of the manuscript.

Funding: The study was funded by Lebanese International University-LIU, Lebanon.

Data Availability Statement: Data sharing is not applicable to this article as no new data were created or analyzed in this study.

Acknowledgments: The authors appreciate the efforts of the anonymous reviewers in improving the quality and presentation of their work. Also, the authors extend their appreciation to Lebanese International University-LIU, Lebanon for funding.

Conflicts of Interest: The authors declare no conflict of interest.

References

1. Lucas, J.M. Counted data CUSUM's. *Technometrics* **1985**, *27*, 129–144. [\[CrossRef\]](#)
2. Vardeman, S.; Ray, D.O. Average run lengths for CUSUM schemes when observations are exponentially distributed. *Technometrics* **1985**, *27*, 145–150. [\[CrossRef\]](#)
3. Joekes, S.; Barbosa, E.P. An improved attribute control chart for monitoring non-conforming proportion in high quality processes. *Control. Eng. Pract.* **2013**, *21*, 407–412. [\[CrossRef\]](#)
4. Wu, Z.; Wang, Q. An np control chart using double inspections. *J. Appl. Stat.* **2007**, *34*, 843–855. [\[CrossRef\]](#)
5. De Araújo Rodrigues, A.A.; Epprecht, E.K.; De Magalhães, M.S. Double-sampling control charts for attributes. *J. Appl. Stat.* **2011**, *38*, 87–112. [\[CrossRef\]](#)
6. Wu, Z.; Luo, H.; Zhang, X. Optimal np control chart with curtailment. *Eur. J. Oper. Res.* **2006**, *174*, 1723–1741. [\[CrossRef\]](#)
7. Woodall, W.H. Control charts based on attribute data: Bibliography and review. *J. Qual. Technol.* **1997**, *29*, 172–183. [\[CrossRef\]](#)
8. Xie, F.P.; Castagliola, P.; Qiao, Y.; Hu, X.; Sun, J. A one-sided exponentially weighted moving average control chart for time between events. *J. Appl. Stat.* **2021**, *49*, 3928–3957. [\[CrossRef\]](#)
9. Gan, F.F. Designs of one-and two-sided exponential EWMA charts. *J. Qual. Technol.* **1998**, *30*, 55–69. [\[CrossRef\]](#)
10. Hamilton, M.; Crowder, S.V. Average run lengths of EWMA controls for monitoring a process standard deviation. *J. Qual. Technol.* **1992**, *24*, 44–50. [\[CrossRef\]](#)
11. Shu, L.; Jiang, W.; Wu, S. A one-sided EWMA control chart for monitoring process means. *Commun. Stat. Comput.* **2007**, *36*, 901–920. [\[CrossRef\]](#)
12. Gan, F.F. Exponentially weighted moving average control charts with reflecting boundaries. *J. Stat. Comput. Simul.* **1993**, *46*, 45–67. [\[CrossRef\]](#)

13. Ali, S.; Pievatolo, A.; Göb, R. An overview of control charts for high-quality processes. *Qual. Reliab. Eng. Int.* **2016**, *32*, 2171–2189. [[CrossRef](#)]
14. Kumar, N.; Chakraborti, S.; Rakitzis, A. Improved Shewhart-type charts for monitoring times between events. *J. Qual. Technol.* **2017**, *49*, 278–296. [[CrossRef](#)]
15. Alevizakos, V.; Koukouvinos, C. A progressive mean control chart for monitoring time between events. *Qual. Reliab. Eng. Int.* **2020**, *36*, 161–186. [[CrossRef](#)]
16. Qu, L.; Khoo, M.B.; Castagliola, P.; He, Z. Exponential cumulative sums chart for detecting shifts in time-between-events. *Int. J. Prod. Res.* **2018**, *56*, 3683–3698. [[CrossRef](#)]
17. Alevizakos, V.; Koukouvinos, C. A double exponentially weighted moving average chart for time between events. *Commun. Stat. Simul. Comput.* **2020**, *49*, 2765–2784. [[CrossRef](#)]
18. Hu, X.; Castagliola, P.; Zhong, J.; Tang, A.; Qiao, Y. On the performance of the adaptive EWMA chart for monitoring time between events. *J. Stat. Comput. Simul.* **2021**, *91*, 1175–1211. [[CrossRef](#)]
19. Rahali, D.; Castagliola, P.; Taleb, H.; Khoo, M. Evaluation of Shewhart time-between-events-and-amplitude control charts for several distributions. *Qual. Eng.* **2019**, *31*, 240–254. [[CrossRef](#)]
20. Rahali, D.; Castagliola, P.; Taleb, H.; Khoo, M.B.C. Evaluation of Shewhart time-between-events-and-amplitude control charts for correlated data. *Qual. Reliab. Eng. Int.* **2021**, *37*, 219–241. [[CrossRef](#)]
21. Shah, M.T.; Azam, M.; Aslam, M.; Sherazi, U. Time between events control charts for gamma distribution. *Qual. Reliab. Eng. Int.* **2021**, *37*, 785–803. [[CrossRef](#)]
22. Saghir, A.; Ahmad, L.; Aslam, M. Modified EWMA control chart for transformed gamma data. *Commun. Stat. Simul. Comput.* **2021**, *50*, 3046–3059. [[CrossRef](#)]
23. Sanusi, R.A.; Teh, S.; Khoo, M.B. Simultaneous monitoring of magnitude and time-between-events data with a Max-EWMA control chart. *Comput. Ind. Eng.* **2020**, *142*, 106378. [[CrossRef](#)]
24. Yang, J.; Yu, H.; Cheng, Y.; Xie, M. Design of gamma charts based on average time to signal. *Qual. Reliab. Eng. Int.* **2016**, *32*, 1041–1058. [[CrossRef](#)]
25. Chakraborty, N.; Human, S.W.; Balakrishnan, N. A generally weighted moving average exceedance chart. *J. Stat. Comput. Simul.* **2018**, *88*, 1759–1781. [[CrossRef](#)]
26. Rao, G.S. A control chart for time truncated life tests using exponentiated half logistic distribution. *Appl. Math. Inf. Sci.* **2018**, *12*, 125–131. [[CrossRef](#)]
27. Wu, S.; Castagliola, P.; Celano, G. A distribution-free EWMA control chart for monitoring time-between-events-and-amplitude data. *J. Appl. Stat.* **2021**, *48*, 434–454. [[CrossRef](#)]
28. Aslam, M.; Jun, C.H. Attribute control charts for the Weibull distribution under truncated life tests. *Qual. Eng.* **2015**, *27*, 283–288. [[CrossRef](#)]
29. Chen, S.; Gui, W. Estimation of Unknown Parameters of Truncated Normal Distribution under Adaptive Progressive Type II Censoring Scheme. *Mathematics* **2020**, *9*, 49. [[CrossRef](#)]
30. Gul, A.; Mohsin, M.; Adil, M.; Ali, M. A modified truncated distribution for modeling the heavy tail, engineering and environmental sciences data. *PLoS ONE* **2021**, *16*, e0249001. [[CrossRef](#)]
31. Santiago, E.; Smith, J. Control charts based on the exponential distribution: Adapting runs rules for the t chart. *Qual. Eng.* **2013**, *25*, 85–96. [[CrossRef](#)]
32. Aslam, M.; Khan, N.; Aldosari, M.S.; Jun, C.H. Mixed control charts using EWMA statistics. *IEEE Access* **2016**, *4*, 8286–8293. [[CrossRef](#)]
33. Rizzo, C.; Di Bucchianico, A. Generalized likelihood ratio control charts for high-purity (high-quality) processes. *Qual. Reliab. Eng. Int.* **2023**, *39*, 523–531. [[CrossRef](#)]
34. Noor, S.; Noor-ul Amin, M.; Abbasi, S.A. Bayesian EWMA control charts based on Exponential and transformed Exponential distributions. *Qual. Reliab. Eng. Int.* **2021**, *37*, 1678–1698. [[CrossRef](#)]
35. Sarwar, M.A.; Noor-ul Amin, M.; Khan, I.; Ismail, E.A.; Sumelka, W.; Nabi, M. A Weibull process monitoring with AEWMA control chart: An application to breaking strength of the fibrous composite. *Sci. Rep.* **2023**, *13*, 19873. [[CrossRef](#)]
36. Ali, S. A predictive Bayesian approach to sequential time-between-events monitoring. *Qual. Reliab. Eng. Int.* **2020**, *36*, 365–387. [[CrossRef](#)]
37. Montgomery, D.C. *Introduction to Statistical Quality Control*, 8th ed.; John Wiley & Sons: Hoboken, NJ, USA, 2019.
38. R Core Team. *R: A Language and Environment for Statistical Computing*; R Foundation for Statistical Computing: Vienna, Austria, 2021.

Disclaimer/Publisher’s Note: The statements, opinions and data contained in all publications are solely those of the individual author(s) and contributor(s) and not of MDPI and/or the editor(s). MDPI and/or the editor(s) disclaim responsibility for any injury to people or property resulting from any ideas, methods, instructions or products referred to in the content.